وزارة التعليم العالي والبحث العلمي

Ministry of Higher Education and Scientific Research

BADJI MOKHTAR-ANNABA

UNIVERSITY

UNIVERSITE BADJI MOKHTAR

ANNABA

جامعة باجي مختار

ـ عنابةـ

Faculty of Sciences

Department of Mathematics

Year: 2024/2025

THESIS

Presented with a view to obtaining the doctorate degree

Identification and Numerical Analysis of Motor-Converter

Stream

Applied Mathematics

Speciality

Differential Equations and Applications

By

GOURI Nesrine

SUPERVISOR: MIHOUB Mohamed Larbi **MCA** **U.B.M. - Annaba**

CO-SUPERVISOR: BENDJAMA Hocine **D.R.** **URMM.CRTI. - Annaba**

In front of the jury

PRESIDENT: TAALLAH Frekh **Prof.** **U.B.M.- Annaba**

EXAMINER: MOUSSAOUI Abdelkrim **Prof.** **U. 8 mai 1945- Guelma**

EXAMINER: ZOUYED Fairouz **Prof.** **U.B.M. - Annaba**

وزارة التعليم العالي والبحث العلمي

Ministère de l'Enseignement Supérieur et de la Recherche Scientifique

BADJI MOKHTAR-ANNABA

UNIVERSITY

UNIVERSITE BADJI MOKHTAR ANNABA

جامعة باجي مختار

ـعنابةـ

Faculté des Sciences

Département de Mathématiques

Année : 2024/2025

THÈSE

Présentée en vue de l'obtention du diplôme de Doctorat

Identification et Analyse Numérique d'un Ensemble Machine-Convertisseur

Filière
Mathématiques Appliquées

Spécialité
Equations Différentielles et Applications

Par
GOURI Nesrine

DIRECTEUR DE THÈSE: MIHOUB Mohamed Larbi **MCA** **U.B.M. - Annaba**

CO-DIRECTEUR DE THÈSE: BENDJAMA Hocine **D.R.** **URMM.CRTI.-Annaba**

Devant le jury

PRESIDENT: TAALLAH Frekh **Prof.** **U.B.M. - Annaba**

EXAMINATEUR : MOUSSAOUI Abdelkrim **Prof.** **U. 8 mai 1945- Guelma**

EXAMINATEUR: ZOUYED Fairouz **Prof.** **U.B.M. -Annaba**

DEDICATION

To my mother, for her love, sacrifice, support and encouragement,

To my father who planted the seed of knowledge in my mind and nurtured it…. His dream came true.

Acknowledgment

First and foremost, I would like to thank God for giving me the strength, knowledge, ability, and opportunity to undertake this research study and to persevere and complete it satisfactorily.

I am immensely grateful to my thesis director, Doctor MIHOUB Mohamed Larbi, for respect, support, encouragement, and insightful feedback has been instrumental over the years. Your keen observations and relevant remarks have profoundly impacted my research journey, and

My sincere appreciation extends to my co-director, Doctor BENDJAMA Hocine, for his outstanding guidance throughout my graduate study. Your invaluable advice over these years has not only aided in shaping my future research career but has also instilled in me the confidence to trust in my capabilities. Your mentorship has been a cornerstone of my development as a postgraduate student, and for that, I am eternally thankful.

A special thanks goes to Professor TAALLAH Frekh, Professor MOUSSAOUI Abdelkrim and Professor ZOUYED Fairouz for their acceptance of the examination of this work.

I wish to express my gratitude to all my teachers from the primary school to the university; I speak of those who gave me knowledge without expecting anything in return, who offered their time and effort to guide me without hesitation, and stood by me at every step. I speak of those whose words were light, whose patience was strength, and whose generosity knew no bounds. Of those with pure hearts and open minds, who ask for no reward or recognition, but share knowledge out of love and deep belief in its purpose…It is of these people that i speak.

Additionally, my appreciation goes out to the Mathematic Department members, for their support and facilitation throughout these years. Their dedication and cooperation played a vital role in sustaining and our journey.

To my brothers, who selflessly stood by my side and sacrificed for my success; thank you for always putting me first and lifting me up so I could reach higher. Your unwavering support means more than words can express. Thank you to the hardships that taught me and to the challenges that shaped me, because without them, I would not have become who I am today.

To my husband, a man of his word-steadfast, reliable, and endlessly supportive. You have stood by me through every challenge, offering strength, deep understanding, and encouragement beyond measure.

To my daughter, "رحمتي" the light of my life, the reason behind my greatest sacrifices and proudest achievements—thank you. Your presence made me stronger, and your love continues to be my greatest source of motivation.

To my family, friends and colleagues, to everyone who has supported me directly or indirectly during this journey, I extend my deepest thanks. Your contributions have not only facilitated this work but have also paved the way for future endeavors. Your support is unforgettable.

تحديد وتحليل عددي لتجميع المحرك والمحول

ملخص

في التطبيقات الصناعية الحديثة، تعتمد موثوقية أنظمة الإنتاج ارتباطًا وثيقًا بأداء الآلات الدوارة التي تعمل بواسطة المحولات الثابتة. توفر هذه التركيبة كفاءة عالية في استهلاك الطاقة، لكنها تتطلب صيانة دقيقة لمنع الأعطال المكلفة. تتناول هذه الأطروحة مشكلة الكشف عن أعطال المحامل، التي تعد من أكثر الأعطال شيوعًا وخطورة في هذه الأنظمة. الهدف الرئيسي هو استخراج معلومات دقيقة تعكس حالة صحة الآلة من خلال تحليل إشارات الاهتزاز. لتحقيق ذلك، تم تطوير منهجية تعتمد على النمذجة الرياضية والتحليل العددي لإشارات الاهتزاز المقاسة. تم اقتراح طريقة جديدة لاستخراج الميزات تجمع بين طريقة إزالة الالتباس باستخدام الحد الأدنى للانتروبيا وخوارزمية فان سيتيرت . تُستخدم تقنية لبناء مرشح عكسي يقلل من تأثيرات التعتيم الناتجة عن مسار الانتقال. ثم تعمل خوارزمية ، المُنظمة بواسطة طريقة تيخونوف-ميلر، على تحسين إعادة بناء المكونات النبضية المرتبطة بالأعطال. تساهم هذه الاستراتيجية المدمجة في تحسين وضوح مؤشرات العطل ودعم الكشف الأدق والأسرع عن الأعطال. تسهم النتائج في تعزيز كفاءة مراقبة الحالة والصيانة التنبؤية للآلات الدوارة المغذاة بواسطة المحولات.

الكلمات المفتاحية: تشخيص الأعطال، الآلات الدوارة، إشارة الاهتزاز، المحمل، إزالة الالتباس، الخوارزميات التكرارية.

Identification et analyse numérique d'un ensemble machine-convertisseur

Résumé

Dans les applications industrielles modernes, la fiabilité des installations de production dépend étroitement des performances des machines tournantes alimentées par des convertisseurs statiques. Cette configuration assure une haute efficacité énergétique, mais impose des exigences strictes en matière de maintenance afin de prévenir des défaillances coûteuses. Cette thèse traite de la détection des défauts de roulements, qui constituent l'une des pannes les plus fréquentes et critiques dans ces systèmes. L'objectif principal est d'extraire des informations pertinentes caractérisant l'état de santé de la machine à partir de l'analyse des signaux vibratoires. Pour ce faire, une méthodologie basée sur la modélisation mathématique et l'analyse numérique des signaux vibratoires mesurés est développée. Une approche innovante d'extraction de caractéristiques est proposée, combinant la déconvolution à entropie minimale (Minimum Entropy Deconvolution – MED) et l'algorithme de Van Cittert (VC). La technique MED permet de construire un filtre inverse réduisant les effets de masquage induits par le chemin de transmission. Ensuite, l'algorithme VC, régularisé par la méthode de Tikhonov-Miller, améliore la reconstruction des composantes impulsionnelles liées aux défauts. Cette stratégie combinée accroît la clarté des indicateurs de défaut et favorise une détection plus précise et rapide des pannes. Les résultats contribuent à l'optimisation des stratégies de surveillance conditionnelle et de maintenance prédictive des machines tournantes alimentées par convertisseur.

Mots-clés : Diagnostic de défaut, Machines tournantes, Signal vibratoire, roulement, Déconvolution, Algorithme itératif.

Identification and numerical analysis of motor-converter

Abstract

In modern industrial applications, the reliability of production facilities is strongly linked to the performance of rotating machines driven by static power converters. This configuration offers high energy efficiency but demands rigorous maintenance to prevent costly failures. This thesis addresses the problem of detecting bearing faults, which are among the most common and critical failures in such systems. The goal is to extract useful information that characterizes the machine's health state by analyzing vibration signals. To achieve this, we develop a methodology based on mathematical modeling and numerical analysis of the measured vibration signal. A novel feature extraction approach is proposed, combining Minimum Entropy Deconvolution (MED) and the Van Cittert Algorithm (VC). The MED technique is used to construct an inverse filter that reduces the masking effects of the transmission path. Then, the VC, regularized using the Tikhonov-Miller method, enhances the reconstruction of impulsive components related to faults. This combined strategy improves the clarity of fault indicators and supports more accurate and timely fault detection. The results contribute to more efficient condition monitoring and predictive maintenance in converter-fed rotating machinery.

Keywords: Fault diagnosis, Rotating machine, Vibration signal, Bearing, Deconvolution, Iterative algorithm.

Table of Contents

List of Figures:

General introduction

In a constantly evolving industrial context, ensuring the reliability and efficiency of production systems has become a critical priority. This need is increasingly addressed through the integration of advanced technologies, including power electronics, microelectronics, and control algorithms [87, 90]. These developments have facilitated the extensive use of machine-converter assemblies; particularly asynchronous machines powered by static converters, which are now essential components in variable-speed applications thanks to their energy performance and operational flexibility. This architecture, recognized for its energy efficiency and control flexibility, nevertheless introduces complex dynamics that make condition monitoring more challenging. Therefore, ensuring effective and predictive maintenance of these systems requires the development of increasingly robust diagnostic techniques.

Common diagnostic tools used in this context include vibration analysis, mechanical deformation studies, thermal flow monitoring, noise analysis, oil analysis, and thermal imaging [12, 20]. Among these, vibration analysis has proven to be one of the most effective techniques for ensuring the reliable operation of rotating machinery. Rotating machines and their components, such as shafts, bearings, and gears, emit characteristic vibratory energy whose properties change significantly when defects occur. Consequently, any degradation in these elements is reflected in their vibration signatures, highlighting the importance of vibration monitoring for the early detection of faults and the prevention of unexpected, costly, and potentially hazardous breakdowns [13, 31 and 63]. The richness of the information contained in vibration signals, particularly in the case of bearing defects, which are both common and critical in modern industrial systems, makes vibration analysis a primary focus of research in condition monitoring. Bearings, in particular, support radial and axial loads in rotating machines [90]. Their performance reflects the performance of the rotating system. Any deterioration can cause serious malfunctions with major economic and safety consequences. Monitoring their condition has therefore become indispensable [17, 87]. Generally, bearing defects can occur on the inner race, the outer race, the rolling element, or the cage. As the rolling element passes over the defect, an impulse signal containing information about the faults is generated periodically, with a time period corresponding to the Bearing Characteristic Frequencies (BCFs). These repetitive

impulses appear as sharp peaks and decay rapidly due to the internal damping of the system, which causes the vibration signals to exhibit amplitude modulation behavior [85]. The periodic impulses are short in duration and are generally contaminated by noise and other vibrational interferences [86].

Early fault diagnosis in rolling bearings using vibration analysis requires signals with sufficient clarity to detect even slight variations caused by defects. However, bearing vibration signal is generally nonstationary, composed of multiple overlapping components, and often heavily affected by noise. In complex machines with multiple elements, this issue is significantly amplified, since each component contributes its own vibrational energy. As a result, when monitoring a particular element, the vibrations generated by other parts affect the signal of interest. Although placing sensors close to the specific component can help mitigate this problem, practical limitations such as component inaccessibility and manufacturer warranty policies often prevent such positioning. Sensors are therefore commonly installed on the outer casing, where they inevitably capture not only the vibrations of the targeted component but also those generated by other parts. This leads to a superposition of vibrational energy from various components, further affected by noise. The dissipation of vibrational energy adds yet another layer of complexity to the signal interpretation. The measured signal thus becomes a mixture of multiple sources, where the signal of interest is further distorted by the transmission path, which represents a convolution operation, making early fault detection a classical ill-posed inverse problem [10, 44, and 58].

The main objective of this work is to address this issue through a mathematical point of view with signal processing tools, focusing on the extraction of relevant features from highly noisy vibration signals. Our approach relies on analytical and numerical techniques capable of enhancing impulsive components characteristic of mechanical faults. A proper understanding of the physical and dynamic mechanisms governing electromechanical systems is essential to ensure reliable interpretation of measured signals and accurate localization of anomalies. In this context, the thesis concentrates on the identification and signal-based analysis of faults in machine–converter systems. The adopted methodology centers on vibration-signal processing to enhance fault-related features efficiently and robustly, even in the presence of significant noise and without requiring detailed knowledge of the complete system dynamics. By emphasizing signal enhancement and feature extraction rather than exhaustive physical modeling, this work

contributes to the development of mathematically grounded diagnostic tools adapted to the complexity of modern electromechanical systems, offering a practical and flexible solution for predictive maintenance and fault detection in industrial environments.

Among the various techniques studied in the literature, Minimum Entropy Deconvolution (MED) has been widely adopted for bearing fault identification [30, 49, 5, and 50]. This interest stems from the fact that vibration signals in bearings contain multiple overlapping components, making the BCFs often difficult to distinguish in the spectrum, which in turn degrades diagnostic performance. To address this issue, signal enhancement methods capable of suppressing noise and emphasizing impulsive features have become essential. In this context, recent studies have increasingly focused on deconvolution-based approaches as a key step toward recovering informative impulses. MED, in particular, is frequently integrated with complementary signal processing techniques to improve the robustness and effectiveness of fault detection. For example, Jiang et al. [43] combined MED with envelope spectrum analysis to enhance the detection of weak faults in rolling element bearings, demonstrating improved condition monitoring capabilities. Had and Sabri [35] proposed a two-stage blind deconvolution strategy, targeting the effective extraction of bearing fault features from noisy vibration signals. Cheng et al. [50] developed an adaptive multipoint optimal MED method, refining the deconvolution process for enhanced fault diagnosis performance in rolling bearings. Zhang et al. [88] introduced an improved maximum correlation kurtosis deconvolution approach tailored for detecting weak faults in planetary gear trains, focusing on increasing sensitivity to impulsive components. In a related contribution, Chen et al. [19] proposed a blind deconvolution method assisted by periodicity detection techniques, specifically aimed at strengthening fault feature extraction in bearing signals.

In this work, we propose a deconvolution strategy designed to enhance the impulsive features associated with bearing faults. The method begins with the application of MED, which optimizes a Finite Impulse Response (FIR) filter by minimizing the entropy of the filtered signal. This step provides an initial inverse filter that highlights the impulsive components generated by bearing defects. Building on the original mathematical formulation, where the measured vibration signal is modeled as the convolution between an underlying impulsive source and the system's transmission function, we address the well-known difficulty that direct inversion of the convolution equation typically leads to unstable or unsatisfactory solutions. To obtain a unique

and stable reconstruction, the initial MED-derived filter, which suppresses the effect of the transmission path and emphasizing fault-related impulses, is subsequently refined using the Van Cittert (VC) iterative deconvolution algorithm [79], implemented within a regularization framework inspired by Tikhonov's method [72]. This iterative refinement allows a more faithful recovery of the source signal by progressively reducing residual distortions and suppressing irrelevant components. After obtaining the final deconvolved signal, the statistical indicator "kurtosis" is computed to assess the enhancement of impulsive features and evaluate the overall quality of the reconstruction. Through this combined MED–VC approach, the proposed methodology overcomes several limitations of conventional vibration analysis by providing a robust, mathematically grounded framework capable of isolating fault signatures in highly noisy and nonstationary environments, thereby enabling reliable early fault detection in complex electromechanical systems.

This thesis is organized as follows:

In the first chapter, we establish the technical and theoretical context for fault diagnosis in converter-fed rotating machines. The chapter begins by defining key terminology and describing the machine–converter architecture, highlighting the effects of power electronics on vibration signal characteristics. It then introduces common mechanical and electrical faults; particularly bearing defects, and presents condition-based maintenance strategies centered on vibration analysis. Finally, it outlines the limitations of classical signal processing methods in noisy, non-stationary environments, thereby motivating the advanced deconvolution techniques developed in the remainder of this work.

The second chapter presents the essential theoretical and methodological foundations necessary for understanding and implementing advanced vibration-based diagnostic techniques. It begins with a detailed overview of the physical and mechanical phenomena underlying faults in machine-converter systems, alongside the fundamental principles of condition monitoring. The chapter then reviews classical vibration analysis methods and their limitations in addressing the complexity of fault signals. To overcome these challenges, it introduces key mathematical concepts related to inverse problems, deconvolution, and regularization, which are crucial for processing noisy signals. Finally, it presents in detail deconvolution techniques; particularly the MED method and the VC algorithm, that form the core of the proposed strategy for extracting fault-related features in bearing diagnosis.

The third chapter is devoted to the application of the proposed method to real and simulated vibration signals. The dataset includes measurements collected from test bench under controlled fault conditions affecting bearing components (outer race, inner race, and rolling element). We apply the combined MED and VC method to these signals and compare the results with traditional diagnostic techniques. The effectiveness of the method is evaluated through kurtosis, to validate the quality of signal enhancement and the clarity of fault features.

Finally, the thesis concludes with a summary of findings, a discussion of the contributions of the proposed approach, and future research directions, including its adaptation to other fault scenarios, other machine types, or integration into online monitoring systems.

Chapter 1: Technical and theoretical context

1 Introduction

This chapter provides the technical and theoretical context necessary for understanding the challenges of fault diagnosis in converter-fed rotating machines. It begins with the definition of key terminology relevant to the field of industrial diagnostics, before presenting a detailed description of the machine–converter architecture. It also discusses the impact of power converters, particularly voltage-source inverters, on the machine's dynamic behavior and on the characteristics of the resulting vibration signals. This is followed by a classification of fault types and an analysis of their physical origins, including mechanical, thermal, electrical, and environmental factors.

The second part of the chapter introduces the fundamental principles of condition-based maintenance and reviews the monitoring tools commonly used in industrial environments. Particular attention is given to vibration analysis, which has proven to be one of the most sensitive techniques for detecting early-stage mechanical defects. The theory of vibration, the structure of the signal acquisition chain, and the characteristics of vibration signals are then presented as a foundation for diagnostic interpretation.

Finally, the chapter examines the limitations of conventional vibration-based diagnostic approaches when applied to converter-fed systems, where complex noise and non-stationary behavior hinder accurate fault identification. These limitations motivate the introduction of advanced deconvolution-based signal processing methods, whose theoretical formulation and implementation are developed in Chapter 2.

2 Terminology and definitions of fault diagnosis

Before going further, it is important to first define and clarify the key terms commonly used in fault diagnosis and condition monitoring:

- **Physical system**

A physical system is a set of interconnected or interacting elements (components, constituents) organized to perform a function [73].

- **Model**

A model of a physical system is a description of its structure and a behavioral or functional representation of each of its components. A behavioral representation consists of relationships between various variables of the system, classically called cause-and-effect relationships. A functional representation is more abstract, since it addresses only the presumed objectives that the physical system must achieve [84].

- **Signatures**

The theoretical signature of a defect can be understood as the expected trace of the fault on the various residual response analyses modeling the system. In other words, the theoretical signature corresponds to the detection results when all tests sensitive to the fault react [72].

- **Signal**

A signal which conveys information, usually about the state or behavior of a system, is mathematically represented as a function of one or more variables [56].

- **Anomaly**

It refers to any observable deviation from the expected behavior of a system, signal, or process under nominal operating conditions. It constitutes an early indicator of abnormal operation, typically detected through statistical or spectral analysis, and does not necessarily imply the presence of a physical defect [73].

- **Fault**

A fault is a physical or functional irregularity within a system component that causes its behavior to deviate from the designed performance. It represents the underlying cause of the observed anomaly and may remain latent or evolve over time toward a critical condition [73, 74].

- **Failure**

A failure is the loss or degradation of a system's ability to perform its intended function within specified performance limits. It denotes the final stage of the degradation process, resulting from the progression of an undetected or uncorrected fault [2, 73].

- **Supervision**

Supervision encompasses three main functions: detection, localization, and decision [73].

- **Detection:** Detection involves recognizing that a device is operating in a faulty mode based on knowledge of certain system characteristics.

- **Localization (Identification):** Localization aims to determine the physical or functional causes of a fault, that is, to identify the component(s) responsible.
- **Decision:** This consists first in determining the operating mode in which the system should be placed (e.g., degraded mode or normal operation). Then, it involves precisely defining the actions required to achieve the chosen mode.

- **Diagnosis**

The term diagnosis can have different interpretations depending on the context and field of application. In the context of industrial processes, diagnosis aims to determine the cause of a fault or failure [2, 23 and 73]. The definition adopted by the international standardization body AFNOR (the standards organization of France [2]) is as follows:

- Diagnosis is the identification of the probable cause of a failure through logical reasoning based on a set of information obtained from inspection, monitoring, or testing.

3 Machine-converter system architecture

The machine–converter assembly, widely used in industrial applications, consists of an asynchronous motor powered by a static power converter, typically a voltage-source inverter. This setup provides precise control of speed and torque through voltage and frequency modulation, enhancing operational efficiency.

The asynchronous machine includes the stator, rotor, and bearings; the latter being critical yet vulnerable components often subject to wear and failure. The static converter delivers variable-frequency signals via high-frequency switching, introducing electrical disturbances such as harmonics and electromagnetic interference. These disturbances interact with the mechanical system, producing coupled effects that influence bearing loads, rotor dynamics, and magnetic behavior. Consequently, diagnostic signals (vibration, current, voltage, and temperature) are often nonlinear and noise-contaminated. Understanding this architecture is the key for effective fault diagnosis. It enables specific signal analysis and supports advanced processing methods that extract and enhance fault-specific features from complex data.

3.1 Constitution of the asynchronous machine

In general, according to the pre-descriptions, the asynchronous machine is composed of three principal components that work together to enable energy conversion and mechanical motion [1, 2, 18], as presented in figure 1.1.

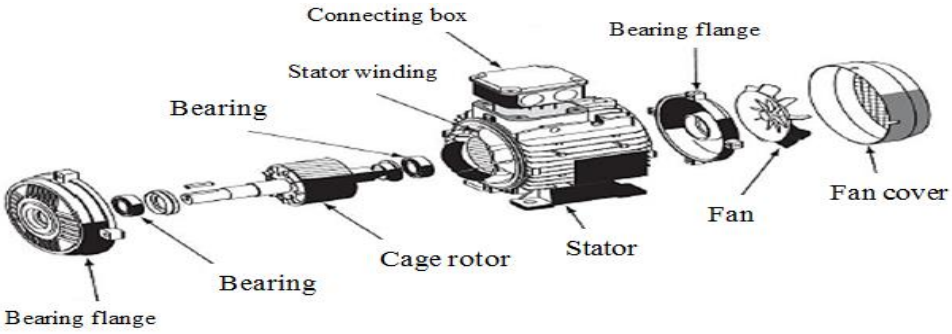

Figure 1.1: Construction of an asynchronous machine

- The stator, the fixed part of the machine to which the power supply is connected.
- The rotor, the rotating part that transmits motion and sets the mechanical load in rotation.
- The bearings, the mechanical part that sets the motor shaft in rotation and drives the loads.

a) Stator

This is the primary, similar to the transformer, fixed, carrying a winding, most often three-phase, housed in slots formed by stacking silicon-coated mild steel sheets (see figure 1.2). It is regularly distributed over the inner face of the stator and connected to the power source. The winding consists of slot conductors and coil heads. The slot conductors create the magnetic field in the air gap that initiates the electromagnetic conversion. The coil heads allow the currents to close by organizing the flow of currents from one slot conductor to the other. The objective is to obtain the most sinusoidal current distribution possible on the surface of the air gap, in order to limit the ripples of the electromagnetic torque [4, 18, 73 and 78].

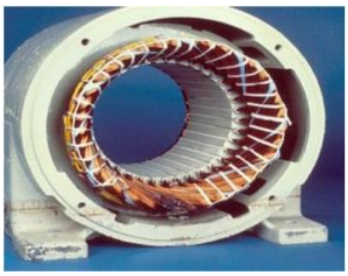

Figure 1.2: Stator

b) Rotor

Movable around the machine's axis of symmetry, it can be both wound and closed on itself or squirrel-cage; (see figure 1.3). In the cage rotor, short-circuit rings allow currents to flow from one rotor bar to the other. These conductive bars are regularly distributed and constitute the rotor

circuit. They are made of aluminum or copper alloy. This cage is inserted inside a magnetic circuit consisting of sheet metal discs stacked on the machine shaft, similar to that of the wound rotor motor [4,18,73,78].

The squirrel-cage motor is simpler to construct than its wound rotor counterpart and, moreover, is more robust. It constitutes the majority of the asynchronous motors currently in service.

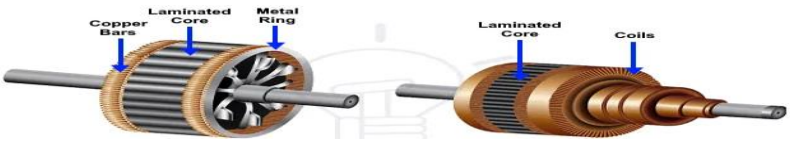

Figure 1.3: Squirrel cage rotor (left) and wound rotor (right)

c) Bearings

Rolling bearing consists of ball bearings and flanges, an inner race and an outer race. The bearings ensure the free rotation of the shaft. The flanges, made of cast iron alloy, are fixed to the stator housing. The assembly thus established then constitutes the asynchronous machine [3, 4, 73, and 78].

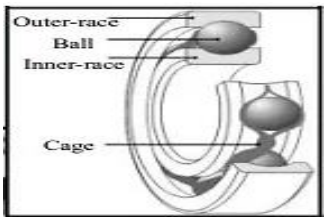

Figure 1.4: Rolling Bearing

3.2 Power supply configuration of an asynchronous motor

The asynchronous motor is typically powered by a static Voltage-Source Inverter (VSI), composed of switching devices such as: Insulated Gate Bipolar Transistors, Metal–Oxide–Semiconductor Field-Effect Transistors, or Gate Turn-Off thyristors [18]. The VSI converts a standard three-phase Alternating Current (AC) supply (220/380 V, 50 Hz) into a variable-frequency, variable-amplitude AC output to control the motor's speed and torque [34].

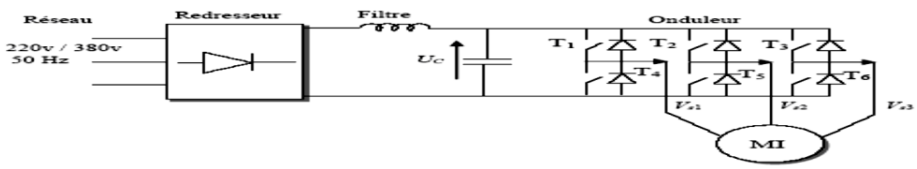

Figure 1.5: Power supply structure of induction machine

As illustrated in figure 1.5, the power supply system includes:

- **AC Source**: Industrial three-phase network;
- **Rectifier**: Converts AC to Direct Current (DC) voltage;
- **Filter**: Reduces ripple and stabilizes the DC bus;
- **Inverter**: Produces Pulse Width Modulation (PWM) controlled AC voltage for the motor.

The inverter's switching introduces high-frequency harmonics, leading to non-sinusoidal voltages and Electromagnetic Interference (EMI). These distortions increase iron and copper losses, stress insulation, and can generate parasitic bearing currents. Such effects degrade machine reliability and contribute to a variety of faults: motor-related (e.g., bearing, stator, rotor), mechanical (e.g., unbalance, misalignment), and electrical (e.g., supply imbalance, converter malfunction). These faults are often interdependent and produce complex, noise-contaminated signals.

Therefore, reliable diagnosis requires precise signal acquisition and advanced processing techniques capable of isolating fault-related features from nonlinear, multi-source disturbances.

4 Faults in induction Machines

4.1 Statistical study

By definition, a failure refers to any incident that leads to abnormal machine behavior and which may, in the short or long term, result in damage and ultimately a complete shutdown of the machine [80].

Despite their robustness, asynchronous machines can exhibit various types of faults, which can be classified according to the statistical study presented below:

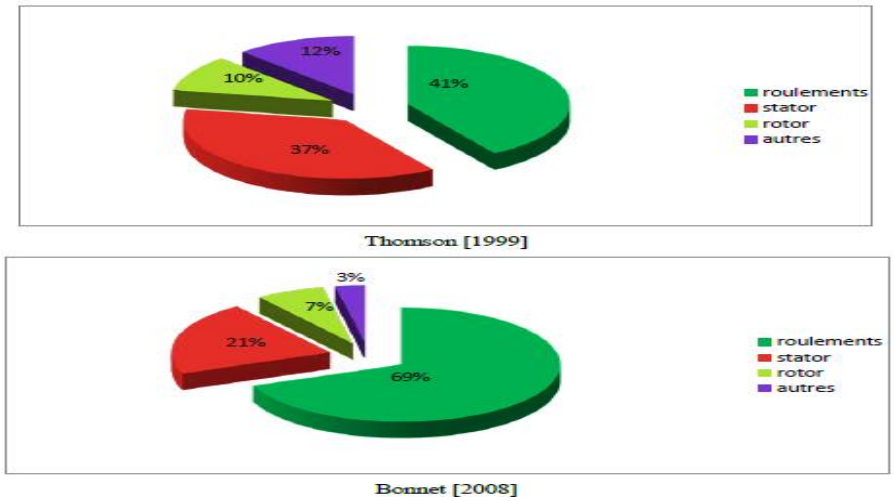

Figure 1.6: Evolution of failure distribution in asynchronous machines over a decade

These studies clearly indicate that most faults originate from bearings, with stator faults occurring less frequently. Advances in manufacturing, especially in insulation materials, have made stator and rotor faults increasingly rare [73].

4.2 Faults classifications

Faults and their causes are numerous, with the most common ones being well-identified [11].These faults can be categorized into two main types: mechanical and electrical. Such faults require special attention, as they can sometimes lead to unexpected machine shutdowns.

4.2.1 Electrical faults

a) Stator faults

The stator suffers from insulation degradation due to thermal, electrical, and mechanical stresses, leading to inter-turn, phase-to-phase, or ground short circuits. These faults create current imbalances, reducing efficiency and causing mechanical vibrations. The majority of stator failures originate from insulation breakdown, making partial discharge monitoring critical for early detection.

b) Rotor faults

Rotor faults in wound rotors are similar to those observed in the stator. In the case of squirrel-cage rotors, the most frequently encountered faults include (see figure 1.9):

- Breakage of one (or possibly several) rotor bars,
- Breakage of the end ring (short-circuit ring).

4.2.2 Mechanical faults

More than 40% of faults in induction motors are mechanical in nature. These may include eccentricity faults, bearing faults, and others [78].

a) Eccentricity faults

The consequences of mechanical defects are generally manifested at the air gap by eccentricity defects [41]. Eccentricity, which refers to the misalignment between the rotor and stator axes, is a phenomenon that evolves over time and is present from the time of machine manufacturing. The ultimate stage of eccentricity is physical contact between the stator and rotor, which leads to rapid machine destruction.

Three types of eccentricity are typically identified, as shown in figure 1.7:

- Static eccentricity: The rotor's axis of rotation is fixed but does not coincide with the stator's axis. This is mainly caused by improper centering of the end bells (bearing housings).

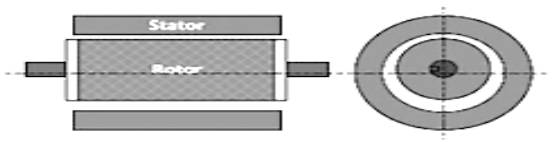

Figure 1.7: Static eccentricity

- Dynamic eccentricity: The rotor rotates around an axis that itself revolves around the geometric axis of the stator. This type is usually due to rotor cylinder deformation, stator cylinder deformation, or degradation of ball bearings.

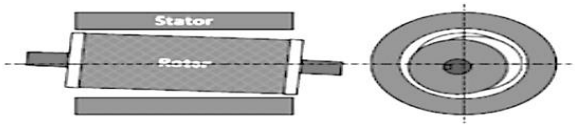

Figure 1.8: Dynamic eccentricity

- Mixed eccentricity: the most common type is a combination of the two previously mentioned forms.

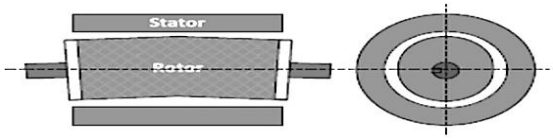

Figure 1.9: Mixed eccentricity

b) Bearing faults

Most faults observed in practice are related to abrasive wear, moisture, corrosion, improper installation, incorrect fits of the rings on the shaft or in the housing, slippage of rolling elements, unexpected contamination, or failure of the cage, seals, or lubrication system, as well as excessive load [78]. These faults lead to mechanical effects in the machines, such as increased noise levels and the emergence of vibrations caused by rotor displacement around the machine's longitudinal axis. Such faults also induce variations (oscillations) in the load torque of the induction machine.

Among all faults affecting induction machines, bearing defects constitute the most common mechanical failures, accounting for more than 40% of reported breakdowns [15, 74, 75]. These defects generally develop progressively and arise from mechanisms such as surface fatigue, contamination, corrosion, improper installation, lubrication problems, or misalignment. As they evolve, bearing faults generate impulsive forces that produce mechanical imbalances, increased vibration levels, torque oscillations, and noise.

In advanced stages, these degradations may lead to severe mechanical malfunction and, in the worst cases, complete machine failure.

Bearings are essential components designed to support radial and axial loads while minimizing friction. Their performance directly influences the reliability of the entire machine system. Common causes of bearing failure include:

- Surface fatigue (spelling or flaking),
- Contamination, moisture or corrosion,
- Lubrication system failure,
- Improper installation or misalignment.

These faults result in impulsive responses, which excite specific frequencies (bcfs) observable through spectral and envelope analysis. Given their critical role and high susceptibility to failure, especially in converter-fed machines, this study places particular emphasis on the detection and identification of bearing faults using advanced signal processing methods designed to extract and amplify defect-related signatures from vibration signals.

The bearing can deteriorate prematurely, leading to surface damage in the form of cracks [42]. These cracks may appear on the surface or may result from a failure in the underlying material layer. This type of failure can be detected in a spectrum by identifying the characteristic

frequencies, which correspond to impact frequencies when a rotating component encounters a defect [43]. The formulas used to determine these frequencies are as follows:

- Outer race fault frequency

$$f_{ORF} = \left(\frac{Nl}{2}\right) f_r \left[1 - \left(\frac{d}{Dl}\right) \mathrm{Cos}\, \varphi\right] \tag{1.1}$$

- Inner race fault frequency

$$f_{IRF} = \left(\frac{Nl}{2}\right) f_r \left[1 + \left(\frac{d}{Dl}\right) \mathrm{Cos}\, \varphi\right] \tag{1.2}$$

- Rolling element fault frequency

$$f_{BF} = \left(\frac{Dl}{d}\right) f_r \left[1 - \left(\left(\frac{d}{Dl}\right) \mathrm{Cos}\, \varphi\right)^2\right] \tag{1.3}$$

- Cage fault frequency

$$f_c = \left(\frac{1}{2}\right) f_r \left[1 - \left(\frac{d}{Dl}\right) \mathrm{Cos}\, \varphi\right] \tag{1.4}$$

In the equations above, Nl represents the number of balls, f_r denotes the rotational frequency, d is the ball diameter, Dl is the pitch diameter of the bearing, and $\propto$ is the contact angle (see figure 1.10).

A theoretical study on bearings made it possible to estimate the service life using the following relation:

$$L_{10} = Kl \left(\frac{Cl}{P}\right)^3 \tag{1.5}$$

Where L_{10}, and P represent the bearing life in millions of revolutions, the rated (basic dynamic) load, and the applied load, respectively. Note that for ball bearings, the exponent $L = 3$.

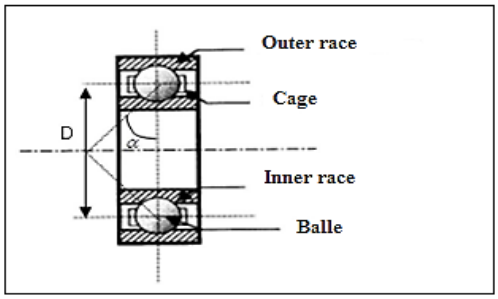

Figure 1.10 : Rolling Bearing

These characteristic frequencies can typically be observed when faults occur on the bearing components. Indeed, impulses are generated each time a rolling element encounters a spall or defect along its path.

4.3 Faults origins

The majority of these faults originate from a combination of various stresses acting on the machine, which can be categorized as thermal, electrical, mechanical, environmental, and manufacturing-related.

- **Thermal:** Excessive temperature rise degrades winding insulation and bearing lubricants, reducing lifespan. Causes include voltage imbalance, poor ventilation, high ambient temperature, frequent restarts, and overloads [1, 11].
- **Electrical stresses:** Overvoltage and fast transients deteriorate insulation through partial discharges. In converter-fed machines, bearing damage can result from shaft currents and electrical arcing [11, 41].
- **Mechanical:** Repeated thermal cycling and vibrations cause insulation cracks, delamination, and abrasion. Contributing factors include misalignment; rotor eccentricity, poor fits, and overloads [12].
- **Environmental:** Moisture, chemicals, and dust accelerate insulation breakdown and bearing wear, leading to electrical leakage and mechanical failure [11].
- **Manufacturing defects:** Poor assembly, faulty welding, and casting flaws can compromise mechanical integrity and electrical reliability from early operation stages [41].

5 Fundamental concepts of maintenance using vibration analysis

In the industrial world, companies primarily seek to maximize their profits. Given the high cost of maintenance operations, it is essential to allocate an optimal maintenance budget. Indeed,

the shutdown of a production machine can result in significant financial losses. Furthermore, a technical fault can negatively affect product quality. Therefore, establish rigorous monitoring in order to quickly detect anomalies and assess the urgency of corrective action.

The evolution of a process over time typically follows three stages: the preparation period leading up to normal operation, the normal operating phase, and the degradation phase (see figure 1.11).

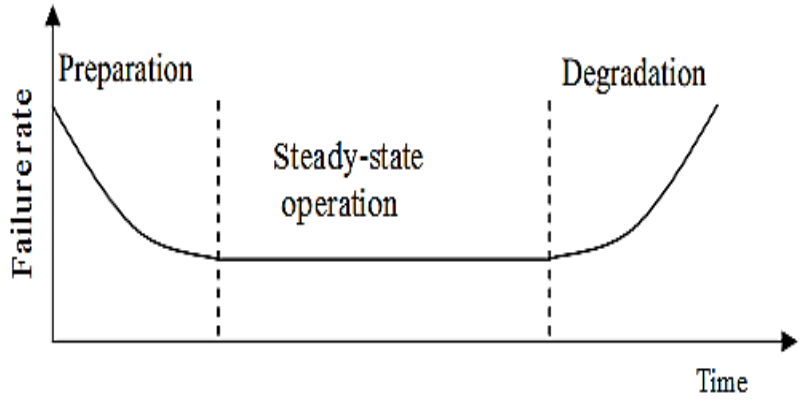

Figure 1.11: Evolution of a process over time

Monitoring aims to ensure the safety and control of operations by using selected indicators such as noise, vibration, or temperature [61, 62, 70 and 84], and it reflects the actual condition of systems. Many researchers have focused on developing monitoring methods for fault detection to reduce productivity losses [67, 27].

Let us introduce some fundamental concepts and definitions in the field of maintenance, covering vibration theory and the main faults that can occur in rotating machinery.

5.1 Maintenance

According to standard NF X60-010 [60], maintenance is defined as the process of assessing and monitoring the operating condition of equipment in order to pre-diagnose issues and optimize its usage within an industrial facility. The objectives of maintenance include:

- Reducing maintenance-related expenses,
- Preserving equipment in optimal operating condition,
- Extending the service life of the equipment,
- Ensuring safe operation by increasing equipment availability at all times,

- Minimizing downtime by maximizing availability at minimal cost,
- Maintaining the full potential of equipment through rapid troubleshooting and replacement at predefined intervals.

5.1.1 Types of maintenance

There are several types of maintenance:

- **Corrective maintenance:** Often essential when maintenance teams must intervene to repair or replace faulty equipment. This approach is suitable when defective components can be easily repaired or replaced, and spare parts are readily available without additional costs.
- **Systematic preventive maintenance:** This strategy focuses on ensuring that machines are functioning correctly and remain in good working condition. The goal of this routine maintenance is to optimize uptime by continuously monitoring the equipment to ensure optimal performance.
- **Conditional preventive maintenance:** This approach is based on monitoring the actual condition of equipment in order to determine the necessary maintenance actions. The principle is that maintenance should only be performed when specific indicators show signs of performance decline or imminent failure.
- **Predictive maintenance:** Predictive maintenance relies on statistical methods and predictive analytics to anticipate potential failures and schedule corrective actions before breakdowns occur [66].

5.1.2 Maintenance strategy

Defining a maintenance policy helps establish the direction of the overall maintenance strategy. It clarifies maintenance expectations in a clear, objective, and measurable manner, guiding the maintenance department's actions toward achieving the desired and necessary outcomes; such as improving business process profitability, reducing downtime and unexpected failures, and implementing appropriate maintenance techniques (preventive, corrective, predictive, conditional, etc.) [83].

Monitoring plays a crucial role in both preventive and predictive maintenance. Where through analyzing key parameters such as vibrations, noise, temperature, or other selected indicators, early warning signs of impending failures or performance degradation can be detected. Such information serves as a critical basis for effective planning and execution of maintenance operations.

5.2 Monitoring tools

Monitoring tools refer to the various technological means used in the industrial sector to monitor equipment. Given the wide range of available options, it is crucial to identify the most relevant parameters for effective maintenance.

In monitoring, the measured parameters play a fundamental role in detecting faults and anomalies. Abnormal variations in parameters such as vibrations, pressure, temperature, or other selected indicators can signal performance issues, mechanical faults, leaks, or other potential errors (see Table 1.1).

Table 1.1 : Fault detection tools [31]

Parameters / Faults	Temperature	Pressure	Oil analysis	Vibration analysis
Unbalance				×
Gears	×	×	×	×
Bearings	×		×	×
Shaft misalignment	×			×
Bearing journal	×		×	×

Table 1.2: Condition monitoring analysis methods [32]

Methods	Key advantages	Preferred applications
Vibration analysis	- Early detection of machine anomalies - In-depth diagnostics, - Continuous monitoring, - Remote condition monitoring.	- Detection of unbalance, misalignment, mechanical looseness, etc.
Oil analysis	-Identifies lubricant contamination before wear occurs, -Particle analysis for fault source identification.	-Verification of lubricant physico-chemical properties, - Wear particle detection.
Infrared thermography	- Rapid equipment inspection, - Immediate results interpretation.	-Detection of overheating-related faults.
Acoustic analysis	- Detection of audible fault signatures, - Continuous tracking.	-Identification of abnormal noises, - Non-destructive testing.

Vibration analysis proves to be a reliable and non-destructive method for detecting most faults, particularly those related to variations in machine vibration levels. This monitoring technique, for rotating machinery, is thus well-justified [20] and well-suited for diagnosing

malfunctions caused by the machine's mobility or structural condition. A change in vibration behavior can reveal almost all defects likely to affect a rotating system, such as imbalance, misalignment, or worn/damaged bearings (see table 1.2). As an example, vibration analysis is appropriate for detecting mobility and structural faults within a specific frequency range, spanning from a few hertz to several kilohertz.

6 Theory of vibration

According to ISO Standard 2041 "Vibration and Shock – Vocabulary" (August 1990), vibration is defined as: A time-varying change in the magnitude of a characteristic quantity describing the motion or position of a mechanical system, where the magnitude alternates above and below a reference or mean value.

In practice, a body is said to be vibrating when it exhibits oscillatory motion around a reference or equilibrium position. These oscillations may be either periodic or aperiodic, such as harmonic or random motions.

A vibration, as illustrated in figure 1.12, is characterized by:

- **Amplitude (A)**: the deviation from the equilibrium point. Several types of amplitude can be defined:
  - Peak amplitude (PA),
  - Peak-to-peak amplitude (PPA),
  - Root mean square amplitude (RMSA).
- **Period (T)**: the duration between two identical successive positions in the oscillatory motion, expressed in seconds.

In the case of a sinusoidal vibration, the various quantities defined previously are described as follows:

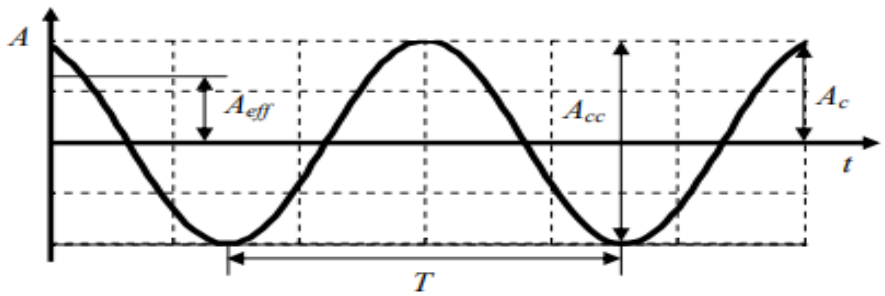

Figure 1.12: Representation of a sinusoidal signal

Vibration is a mechanical phenomenon in which oscillations occur around an equilibrium point, resulting in a change in a motion parameter over time (see figure. 1.13). These oscillations can be either periodic or random, such as the motion of a pendulum or a tire moving over a gravel road.

While some vibrations are desirable, like those produced by a tuning fork, the reed of a wind instrument, or a loudspeaker cone, in many cases, vibrations are unwanted. They can lead to energy losses and produce unpleasant noise. Vibratory motions of engines, electric motors, or any mechanical device in operation are generally considered undesirable. They can be caused by imbalance in rotating components, irregular friction, or poor meshing of gear teeth. Advanced mechanical researchs typically aim to minimize these unwanted vibrations.

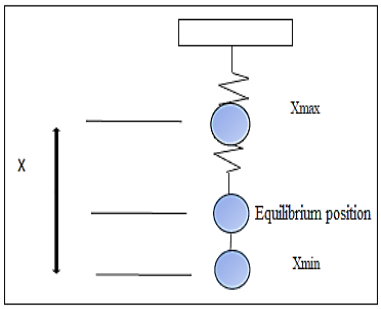

Figure 1.13: Vibration example [91]

Several measures can be used to characterize different types of vibration. These can be represented in two different ways: time or frequency.

6.1 Vibration characteristics

Figure 1.14 shows the time-domain vibration response of an excited mass-spring system. This response takes the form of a sinusoidal function:

$$x(t) = A\,\mathrm{Sin}(\omega t) \tag{1.6}$$

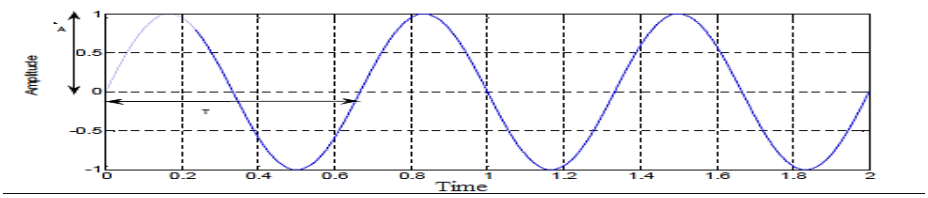

Figure 1.14 :Vibration parameter [91]

Where:

- $x(t)$ *Is* the instantaneous value,
- A is the maximum value of the variable *x(t),*
- T defined as the time interval after which the variable *x(t)* returns to the same value and direction (unit: second [s]).
- F is a frequency, expressed in units of measurement Hertz [Hz]:

$$f = \frac{1}{\mathrm{T}} \tag{1.7}$$

ω is the angular frequency (also called angular velocity), expressed in radians per second [rad/s]:

$$\omega = 2\pi f \tag{1.8}$$

6.1.1 Natural frequency

The natural frequency f_p Of a mass-spring system is the frequency at which the system tends to oscillate freely when disturbed, without any external force applied. For a simple mass-spring system, it is given by:

$$f_p = \frac{1}{2\pi}\sqrt{\frac{k}{m}} \tag{1.9}$$

Where k is the stiffness of the spring and m is the mass [10].

6.1.2 Resonance

When a sinusoidal force of frequency *f* and constant amplitude A is applied to a system, the system's vibration amplitude naturally increases, reaching a maximum when the excitation frequency approaches the system's natural frequency f_p, a condition known as resonance. When a resonant system is subjected to an external excitation close to its natural frequency, it can accumulate energy. The system will begin to oscillate, reaching an equilibrium state influenced by its dissipative elements. However, if damping is insufficient, resonance may lead to system failure [10].

6.2 Vibration modes

Rotating machinery is generally subject to harmonic, periodic, or aperiodic vibrations [91]:

6.2.1 Harmonic vibrations

Simple harmonic motion is a type of linear vibratory motion in which the acceleration of the mass is proportional to its displacement and opposite in direction (see figure 1.15).

This motion is periodic, with constant amplitude, and the velocity is proportional to the body's displacement from the equilibrium position, always directed toward it.

The amplitude of the vibration is always positive and the characteristics of the motion are described by its period (time required to complete a vibration), its frequency (number of vibrations per second) and its phase (determined by the initial conditions of the motion) on the sinusoidal curve. The period and the frequency are constant [91].

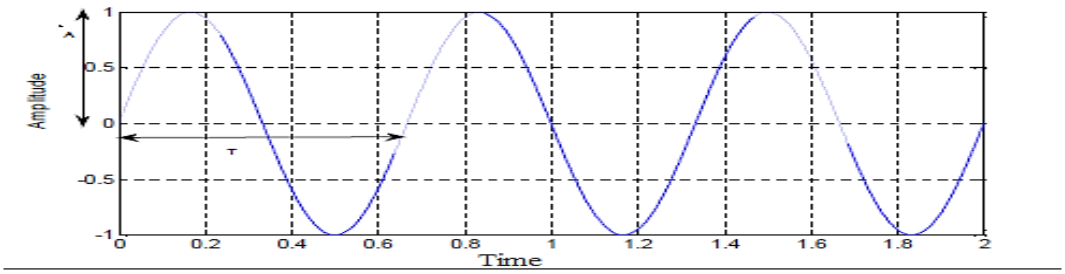

Figure 1.15: Harmonic vibration [10]

6.2.2 Periodic vibrations

These vibrations result from the combination of several harmonic vibrations. They recur at a defined time interval known as the period and are generated by the application of a periodic force intended to excite the system and induce motion [10].

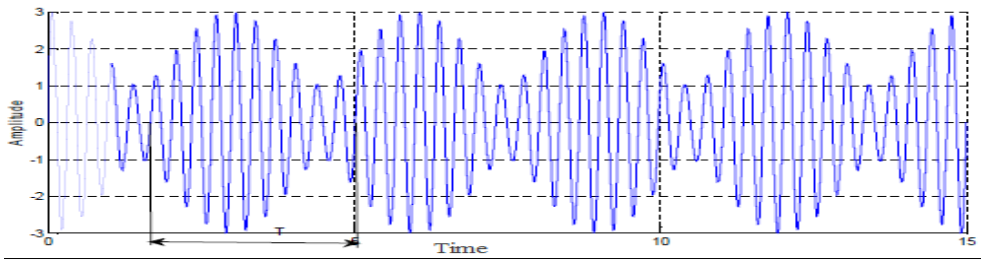

Figure 1.16: Periodic vibration [10]

6.2.3 Aperiodic vibrations

A large class of environmental vibrations, perhaps the most common are aperiodic or even random, meaning they can only be statistically described. Aperiodic vibration is the most fundamental physical representation of "noise." In terms of frequency content, aperiodic vibrations have their energy more or less continuously distributed over a range or band of frequencies [91].

6.3 Vibration signature

Vibrations carry information that allows describing the operating condition of the analyzed machine. By examining these mechanical vibrations, it is possible to assess the remaining lifespan of mechanical components [77], because the ideal machine, which is in good condition, does not vibrate, or the vibration level is low. Low vibrations dissipate in the structure, and they are not remarkable. However, when the machine operates for a long time, stresses and fatigue begin to appear on the machine components, such as gears, bearings, shafts, seals, and bearings. These wear out, and changes occur in their dynamic characteristics. All these factors lead to an increase in energy and vibration levels, and thus defects begin to appear. Therefore, vibration measurements are regularly used as a means of assessing the health of machines. To facilitate the measurement of vibrations of elements subjected to periodic stresses, for example, bearing supports, which are generally accessible from the outside, the vibration signal can be measured as acceleration, velocity, or displacement [89]. With these measurements, the history of fault development can be obtained and compared to a reference level generated by the vibrations of the machine in good condition. Thus, the condition of the machine can be described quickly and at any time [27].

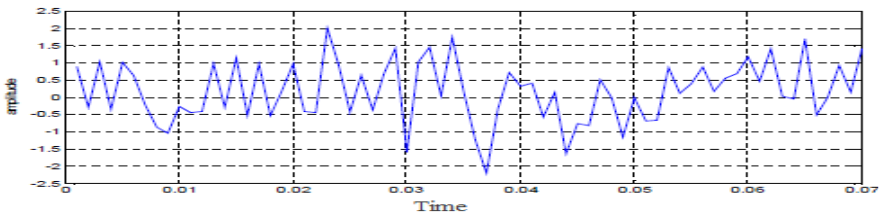

Figure 1.17: Aperiodic vibration [34]

6.4 Relationship between mechanical components and characteristic frequencies

Each rotating mechanical component is associated with a specific vibration level and a characteristic frequency. Analyzing the motion of a rotating machine makes it possible to predetermine the characteristic frequency regions caused by mechanical faults.

7 Vibration signal processing

A defect can be defined as any variation in the nominal functioning of a component, compromising its ability to perform its function effectively. Because of their crucial relevance and vulnerability to mechanical, thermal, or dynamic loads, bearings require specialized

monitoring techniques in order to identify early degradation indicators. The high frequency of bearing failures makes their monitoring essential. This includes the use of signal analysis techniques to detect anomalies and signs of failure. This is precisely the objective of condition-based maintenance, which relies on the monitoring of component health.

Among the available monitoring techniques, vibration analysis has established itself as a particularly effective diagnostic tool. It enables the early detection of mechanical faults by analyzing variations in the vibration signals generated by moving parts, thereby preventing critical failures. This method, both non-intrusive and sensitive, is widely used in industry due to its effectiveness in monitoring rotating components, especially bearings. It enables the identification of various fault types, such as imbalance, misalignment, or internal damage to rolling elements.

However, in systems powered by converters, vibration signals become more complex to interpret. Converters introduce additional disturbances such as frequency harmonics, electromagnetic noise, and nonlinearities from power electronics, which make classical diagnostic methods less reliable. Moreover, traditional signal processing methods show their limitations in complex industrial environments.

7.1 Vibration monitoring and measurement

Monitoring based on vibration analysis involves the following steps:

7.1.1 Data acquisition

The key element in data acquisition is a sensor exposed to vibrations. It converts mechanical effects into a preamplifier electrical signal of vibratory form [62]. This signal is then received by a synchronous sampling unit, amplified by a signal amplifier, and transmitted to data recording software. This process is referred to as the digitization of the data to be processed [69].

7.1.2 Signal conditioning and pre-processing

Once the raw vibration data are acquired, they must undergo conditioning and pre-processing before any diagnostic interpretation can be performed. This stage is essential to improve signal quality, remove unwanted noise, and prepare the data for subsequent analysis.

Signal conditioning generally includes amplification, filtering, and normalization to ensure that the recorded signal accurately reflects the machine’s dynamic behavior within the desired

frequency range. Pre-processing operations may also involve resampling, detrending, or baseline correction, which eliminate artefacts introduced by sensors or acquisition hardware. From a broader perspective, signal processing constitutes a discipline dedicated to the analysis, transformation, and interpretation of various types of signals; acoustic, mechanical, or electromagnetic [32]. Applied to vibration monitoring, it plays a crucial role in extracting relevant information hidden within noisy data, revealing valuable indicators of the machine's mechanical health and facilitating the early detection of incipient faults.

7.1.3 Detection

In this step, the main objective is to detect faults by observing the evolution of the process, which makes it possible to distinguish between normal and abnormal situations [89]. By using detection techniques such as signal analysis, it becomes possible to identify abnormal behaviors such as excessive vibrations, frequency variations, noise spikes, or changes in acoustic signatures.

7.1.4 Diagnosis

Diagnosis aims to identify the cause of a malfunction or problem based on symptoms revealed through observations, examinations, or tests, and to determine its severity. Generally, the diagnostic process follows the detection of an anomaly, as illustrated in figure 1.18 [52].

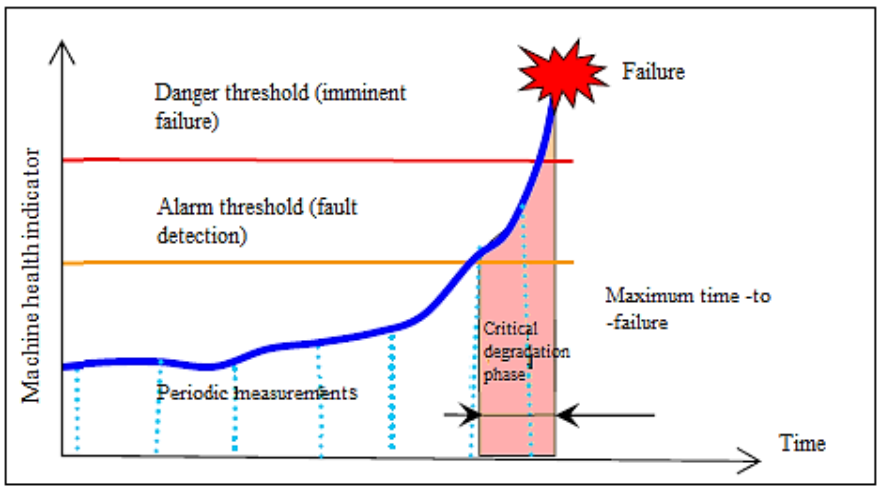

Figure 1.18: Machine health indicator over time

To establish a diagnosis, at least two thresholds must be defined, as illustrated in figure 1.18.

Alarm threshold: At this stage, the indicator informs the presence of a fault, indicating that maintenance will be required. It is important to schedule the machine to shut down at a certain time to minimize production losses.

Danger threshold: At this point, immediate action is necessary, and the defective mechanical component must be replaced, as the system is approaching a failure threshold. Intermediate thresholds can also be defined to refine the analysis.

7.2 Vibration measurement parameters

To analyze the vibrations generated by dynamic forces within machines, three fundamental quantities are typically considered. These quantities are interconnected, as summarized in the following table:

Table 1.3: Vibration measurement parameters [2]

Parameters	**Characteristics**
Displacement [µm, micrometer]	- Low frequencies, - Slow, - Frequency ≤ 100 Hz.
Velocity [mm/s]	- Higher speed, - Reduced displacement, - Slightly higher acceleration, - 100 Hz < Frequency ≤ 1000 Hz.
Acceleration [m/s^2 or g] ; 1 g = 9,81 m/s^2	- Minimal displacement, - Medium velocity, - Highest acceleration, - Broad frequency band, - (0 Hz ≤ Fréquence ≤ 20 khz).

The selection of one of the quantities listed in the table above is crucial for the quality of the diagnosis. This choice depends on the characteristics of the vibration signal, as outlined in Table 1.3. In the presence of a purely sinusoidal vibration, the displacement, velocity and acceleration measurements are interrelated by the following mathematical expressions:

$$V_e = \frac{A_{Cc}}{2\pi f} \tag{1.10}$$

Where V_e denotes velocity and A_{cc} represents acceleration.

$$D_P = \frac{Acc}{2\pi f} \tag{1.11}$$

$$D_P = \frac{Acc}{(2\pi f)^2} \tag{1.12}$$

Where D_p denotes the displacement of the vibratory motion.

To detect low-frequency phenomena, displacement is the preferred quantity, whereas for high-frequency phenomena, such as bearing defects, acceleration is typically selected. Choosing the appropriate measurement quantity is essential to ensure diagnostic quality and depends on the characteristics of the vibration signal [52].

7.3 Measurement chain

The measurement chain consists of several components, including a vibration sensor such as a proximity probe, a velocimeter, or a piezoelectric accelerometer (see figure 1.19). The data acquisition system includes a signal amplifier and an analog filter to limit the bandwidth of the high-frequency components of the signal. The analog-to-digital conversion of the vibration signal is performed by an electronic interface card. The digitized signals are processed using dedicated software that enables filtering, correction, and statistical evaluation. The measurements can be displayed on the input/output interface of a computer.

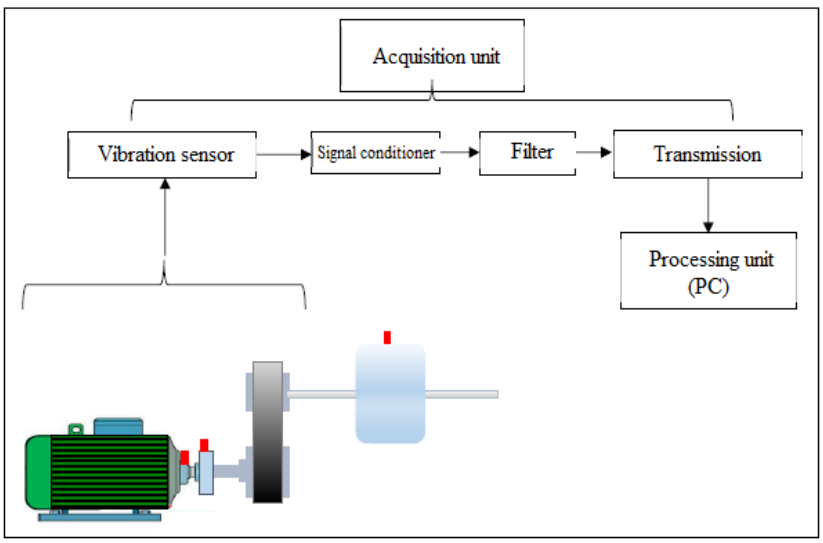

Figure 1.19: Vibration signal measurement chain

7.4 Sensors for vibration measurement

There are several types of sensors: displacement sensors, velocity sensors, and acceleration sensors.

7.4.1 Displacement sensor

Displacement sensor is a device used to measure the distance between the sensor and a target object by detecting the amount of movement and converting it into a distance value (see figure 1.20(a)). Its operating principle relies on an oscillating circuit that produces a sinusoidal magnetic field within the sensor coil. When a conductive object approaches the sensor, eddy currents are induced in the object, causing a loss of electrical energy. This loss is reflected back to the signal conditioner as a voltage variation [70].

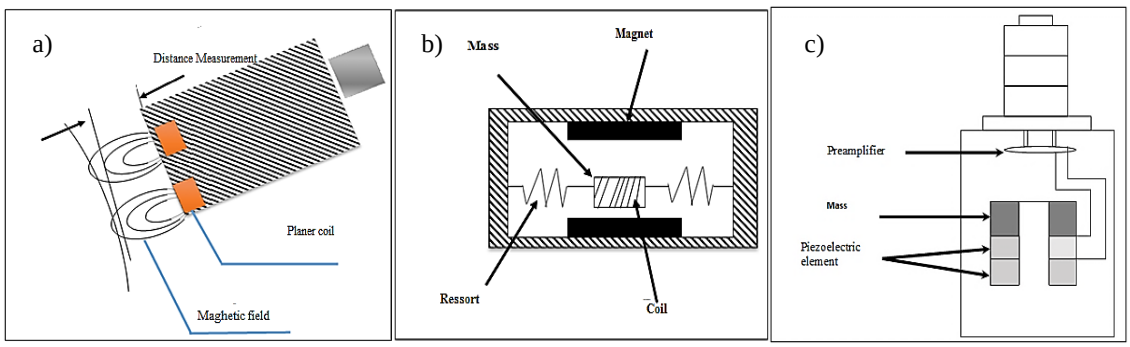

Figure 1.20: (a) Displacement, (b) Sensor velocity and (c) Sensor accelerometer

7.4.2 Velocity sensor

A velocity sensor measures the absolute speed of vibration and provides an electrical signal proportional to this velocity. It consists of a coil suspended by springs and a permanent magnet fixed to the sensor housing with a seismic mass (see figure 1.20(b)). The permanent magnet generates a strong magnetic field around the coil. When the machine to which the sensor is attached vibrates, the permanent magnet follows the vibration movement while the coil remains stationary. This vibration movement induces a voltage difference that depends on the coil's velocity [37].

7.4.3 Accelerometer

An accelerometer generates an electrical signal proportional to the experienced acceleration , due to its piezoelectric disc (quartz), which behaves like a spring, and its preloaded seismic mass (see figure 1.20(c)). The seismic mass moves in response to acceleration, exerting an alternating

pressure on the piezoelectric disc, producing a voltage variation proportional to the applied force and, consequently, to the acceleration of the mass [61].

However, accelerometers are frequency-dependent and are better suited for measuring inertial vibrations where the forces involved are critical. Higher-frequency vibrations produce greater accelerations, resulting in stronger signal levels, whereas lower-frequency vibrations may generate weak signal levels, making it difficult to distinguish useful signals from background noise.

Moreover, the use of accelerometers on smaller objects can be limited because their attachment may modify the object's mass and its natural resonance frequencies. Nevertheless, for larger objects vibrating at higher frequencies, where inertial forces dominate, accelerometers are an excellent choice.

7.5 Selection of measurement points

The placement of the accelerometer must be carefully selected to ensure it is positioned as close as possible to the component being monitored, ideally at the machine's bearing locations, while also providing a direct path for the transmission of vibrations [70].

7.6 Sensor mounting

An optimal mounting arrangement significantly enhances measurement accuracy. For optimal performance, particularly at high frequencies, the base of the accelerometer and the test surface must be clean, flat, smooth, and free from scratches or burrs. To minimize errors caused by unwanted sensor vibrations, a symmetrical mounting configuration is recommended. The mass of the sensor, including all mounting components, should be small relative to the test object ideally; the sensor should not exceed 10% of the object's mass [16]. The sensor axis and the measurement direction should be as closely aligned as possible, especially in the presence of large-amplitude transverse vibrations. When using a threaded screw mount, it is essential to ensure that the screw does not exceed the depth of the threaded hole and that there is no gap under the sensor. The recommended accelerometer mounting methods include: fixing the sensor onto a stud pre-installed on the structure under test, using an isolating clamp or adhesive pad, magnetic base, adhesive (epoxy, wax, double-sided tape, etc.), and mobile phone socket.

Accurate mounting and proper sensor selection ensure high-quality vibration data. However, even under optimal measurement conditions, interpreting vibration signals in converter-fed

environments remains challenging. The following section examines these limitations and motivates the adoption of advanced diagnostic tools.

8 Limitations in real industrial environments and the case of existing bearing faults

In real-world industrial environments; particularly within converter-fed machine systems, vibration analysis faces specific and recurring challenges that significantly hinder signal interpretation [73]. The presence of multiple sources of disturbance deteriorates the quality of vibratory data and limits the reliability of conventional diagnostic tools [9, 53]. The most notable interfering factors include:

- Non-stationary behavior, resulting from variations in speed or load torque, which continuously shift the spectral content of the signal [5];
- Electromagnetic noise, emitted by the power electronics components of the converter, which masks the mechanical fault signatures [34, 80];
- Voltage and current harmonics, introduced by modulation strategies, which create spectral pollution and degrade frequency resolution [12].

These interferences make the extraction of fault-related signatures more difficult, even when the bearing already presents a fault that produces measurable impacts. In such environments, impulses are often submerged in the noise floor, rendering classical detection methods like envelope analysis or kurtosis ineffective [68]. Consequently, detection necessary for proactive and predictive maintenance becomes compromised.

Existing bearing faults generally manifest as transient impulses generated by localized interactions between rolling elements and surface anomalies on the raceways. These fault-induced signals possess several challenging characteristics:

- They are non-periodic and sparse,
- They have very short durations,
- They are deeply embedded in structural and electromagnetic noise,
- Their spectral footprint is often invisible in classical FFT spectra.

Even robust statistical tools such as kurtosis, crest factor, or envelope detection may fail to identify these impulses when the signal-to-noise ratio is unfavorable or when the recurrence frequency of impacts is masked. These limitations call for more selective and noise-resilient

signal processing methods capable of revealing impulsive events within complex and contaminated datasets.

Classical signal processing techniques, despite their historical significance, present inherent limitations that become particularly acute in modern industrial environments. They exhibit high sensitivity to noise and non-stationary conditions, their effectiveness often relies on the assumption of signal stationarity, and they usually require a priori knowledge of the fault frequency band.

These limitations are particularly constraining in machine–converter systems, where the dynamic behavior is non-linear, time-varying, and often unpredictable. In such configurations, vibration signatures generated by existing faults may be distorted, attenuated, or partially masked by convolution effects and electromagnetic interference. These conditions highlight the importance of robust methods capable of extracting fault-related information despite noise, modulation effects, and structural distortions.

Thus, the necessity for advanced diagnostic tools becomes evident. Deconvolution techniques, in particular, offer a powerful framework for this purpose.

8.1 The impact of the MED and VC algorithm

Why use MED and VC?

In a bearing system, the measured vibration signal is composed of fault-induced impulses, the effects of the system's transmission path, and additive noise. This mixture makes it difficult to isolate the fault-related components directly.

In this work, the MED method is employed to estimate an optimal inverse filter FIR. MED iteratively computes the filter coefficients from the measured signal, based on its statistical properties, until convergence to a filter that effectively represents the system's transmission path. The FIR filter obtained through MED forms a key component for subsequent signal processing, serving as the foundational tool to partially undo the convolution effects that have blurred the original fault impulses. This approach is fully data-driven, requiring no prior knowledge of the system or predefined frequency bands, making it suitable for complex and variable industrial environments.

The VC algorithm is a classical iterative deconvolution technique. VC uses the FIR filter estimated by MED iteratively to refine the signal, progressively removing residual convolution

effects and mitigating the smearing of impulses caused by the transmission path. By repeating this process, VC enhances the clarity and temporal resolution of transient events, making the fault-related impulses more distinguishable.

The combination of MED and VC thus enables the progressive reconstruction of true fault-related events, transforming previously blurred or obscured signals into clear, interpretable signatures suitable for reliable diagnosis. This synergistic use of both algorithms provides a robust and innovative framework for fault feature enhancement in complex vibration environments.

9 Conclusion

The analyses and challenges outlined in this chapter highlight the pressing need for advanced signal-processing strategies in the context of modern industrial diagnostics. Classical tools, though foundational, are increasingly limited when confronted with the non-stationarity, noise, and convolution effects characteristic of converter-fed machine systems. In such environments, deconvolution-based techniques, particularly the combined use of MED and VC algorithm, provide powerful means for uncovering weak and obscured fault signatures.

The following chapter builds upon these findings by developing the theoretical and mathematical framework underlying the proposed diagnostic strategy. It focuses on the formulation of the inverse problem, introduces the principles of regularization, and details the implementation of MED and VC techniques for the extraction of incipient bearing-fault signatures from complex vibration signals.

Chapter 2: Advanced signal processing methods for bearing fault diagnosis: a deconvolution-based approach

1 Introduction

This chapter establishes the theoretical and methodological foundations for vibration-based bearing fault diagnosis, focusing on deconvolution techniques to address the inverse problem of impulse recovery. Early fault detection in rotating machinery remains a key challenge due to the complex nature of vibration signals, which are fundamentally convolved with the system's transmission path and further contaminated by noise and competing dynamics. This scenario presents a classical inverse problem that is ill-posed, where recovering the original fault-induced impulses from measured vibrations requires specialized signal processing approaches. To overcome these difficulties, numerous advanced signal processing methods have been developed in recent decades. In this work, we propose a robust approach combining two key deconvolution techniques; the MED and the VC algorithm based on Tikhonov regularization.

As discussed in the previous chapter, vibration-based diagnosis in converter-fed systems often suffers from instability and non-uniqueness in signal reconstruction, emphasizing the need for regularized deconvolution frameworks. Accordingly, this chapter begins with a review of vibration signal analysis fundamentals, followed by the mathematical formulation of the deconvolution problem and its regularization. The final sections detail the MED and VC algorithms, which together constitute the foundation of the proposed hybrid diagnostic approach.

2 Vibration signal analysis techniques

Before introducing the mathematical deconvolution framework, it is important to recall the main aspects of vibration signal acquisition and interpretation, since they provide the basis for understanding the subsequent analytical developments.

2.1 Sampling of a vibration signal

To achieve optimal fault detection performance, special attention must be paid to the sampling frequency, which determines the frequency content available in the measured signal (see Figure 2.1). If the sampling frequency is not properly selected, valuable information

contained in the high-frequency band may be lost, leading to inaccurate diagnosis results. According to the Nyquist theorem (also known as the Shannon sampling theorem), the sampling frequency must be at least twice the highest frequency component present in the signal. In practice, however, a safety margin is commonly applied to this theoretical limit [67], leading to:

$$F_s \geq 2.56 * F_{max} \tag{2.1}$$

Where F_s and F_{max} are the sampling frequency and the maximum frequency of the signal respectively, in hertz. On the other hand, we have:

$$F_s = \frac{1}{T_s} \tag{2.2}$$

Where T_s is the sampling period.

It should be noted that the data acquisition time T_{acq} is the duration used to record measurements of the signal:

$$T_{acq} = N_e T_s \tag{2.3}$$

In Eq. (2.3), N_e represents the number of recorded points.

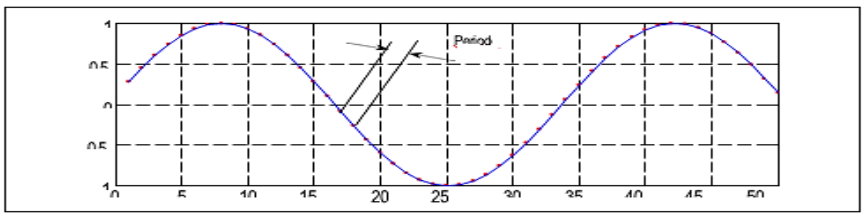

Figure 2.1: Signal discretization

2.2 Resolution of a vibration signal

When collecting vibration data, it is important to first identify the frequencies of interest [67] and then select an appropriate combination of maximum frequency F_{max} and frequency resolution to ensure that all relevant information is captured. Frequency resolution determines the ability to distinguish closely spaced spectral components; higher resolution allows for better separation of nearby frequencies. The frequency resolution of the vibration spectrum is given as follow:

$$\Delta f = \frac{F_{max}}{N_l} \tag{2.4}$$

$$N_l = \frac{N_e}{2.56} \tag{2.5}$$

Where Δf is the frequency resolution, and N_l is the number of spectral lines.

2.3 Vibration analysis techniques

Vibration analysis techniques commonly employ advanced signal processing methods, which are generally divided into two main categories based on the variety of available tools [72]: time-domain and frequency-domain approaches.

2.3.1 Time-domain approach

This method enables the detection of faults but is unable to precisely locate them within the equipment. It relies on analyzing the collected signal from a statistical point of view. When the values of associated indicators are high, the risk of fault development increases [46]. Several time-domain indicators exist; as an example, we can mention:

- **Root mean square (RMS) value**

The most relevant value for assessing the destructive potential of a vibration is generally the Root Mean Square (RMS) value, as it is directly related to the energy content of the vibrations. It takes into account the time history of the waveform, which makes it particularly useful [59]. The mathematical formula used to calculate this value is defined as follows:

$$V_{eff} = V_{RMS} = \sqrt{\frac{1}{N_e}\sum_{n=1}^{Ne}[s(n)]^2} \tag{2.6}$$

In Eq. (2.6), *s(n)* denotes the measured signal.

The RMS value helps detect bearing degradation. However, this value does not allow for the detection of the initial peaks in the signal that occur in the early stages of a fault, and furthermore, it is not possible to accurately identify the fault location. Nevertheless, it does allow for assessing the severity of the defect. It is crucial to note that the RMS value is not sensitive to short-term transient changes, which last only a few milliseconds.

- **Crest factor (CF)**

The CF parameter is commonly used to characterize vibration data. By definition, it is the ratio between the peak value of the signal and its RMS value. For bearings in good condition, CF values generally range between 2.5 and 3.5, but they increase in the presence of defects [15]. CF is mathematically defined as follows:

$$CF = \frac{sup|s(n)|}{\sqrt{\frac{1}{Ne\sum_{n=1}^{ne}|s(n)|^2}}} \tag{2.7}$$

When bearing deterioration begins to appear, the CF value increases, the effective value RMS stays relatively constant [15].

- **Kurtosis**

Kurtosis is sensitive to impulsiveness and allows for the detection of vibration signals associated with defects from their early stages [61]. It is calculated as follows:

$$\text{Kurtosis} = \frac{M_4}{M_2^2} = \frac{\frac{1}{N_e}\sum_{n=1}^{N_e}(s(n)-\bar{s})^4}{\left[\frac{1}{N_e}\sum_{n=1}^{N_e}(s(n)-\bar{s})^2\right]^2} \tag{2.8}$$

In this equation, *s(n)* denotes the time-domain signal, $\bar{s}$ is the mean, and N_e is the length of the signal. Kurtosis is sensitive to mechanical shocks [66].

- **Standard deviation**

This is a measure of variation around the mean. A low standard deviation indicates a tighter distribution of values. Standard deviation can be used as an indicator for the early detection of bearing faults [63]. It is defined as:

$$\sigma = \frac{1}{N_e}\sum_{n=1}^{N_e}(s(n) - \bar{s})^{0.5} \tag{2.9}$$

Where $\bar{s}$ is the mean value.

- **Dissymmetry**

Dissymmetry quantifies the asymmetry of the vibration signal through the probability density function. It is defined as the lack of symmetry in the distribution of values. This dimensionless measure indicates the degree to which the signal is asymmetric around its mean (Eq. (2.10)). If the signal is symmetric, the dissymmetry is zero. Most vibration signals have a symmetric

probability distribution, such as the normal distribution [64]. Thus, a non-zero offset generally indicates an anomaly in the signal.

$$Dissymmetry = \frac{\frac{1}{N_e}\sum_{n=1}^{N_e}(x(n)-\bar{x})^3}{\left[\frac{1}{N_e}\sum_{n=1}^{N_e}(x(n)-\bar{x})^2\right]^{3/2}} \tag{2.10}$$

2.3.2 Frequency-domain approach

This approach is based on the Fourier Transform (FT) of the time-domain signal. Frequency analysis is an effective method for processing vibration signals [70]. By identifying the characteristic frequencies of signal, this method allows for the localization and identification of faults. Spectral analysis serves as the basic tool for processing vibration signals, relying on the FT to transition from the time domain to the frequency domain. It provides valuable information that helps in diagnosing problems at an early stage. By comparing the obtained frequencies with theoretical frequencies, faults can be localized [60]. The following equation defines the FT:

$$S(f) = \int_{-\infty}^{+\infty} s(t)e^{-j2\pi ft}dt \tag{2.11}$$

Where *S(f)* is the FT of s*(t)*, *t* is time, and *f* is frequency. The discretization of the FT from equation (2.11) is:

$$S(k\Delta f) = \frac{1}{N_s}\sum_{n=0}^{N_s-1} s(nt_s)\, e^{-j2\pi k\,\frac{n}{N}}dt \tag{2.12}$$

Where $S(k\Delta f)$ is the discrete FT, t_s is the sampling period of the time-domain signal, *n* is the sample identifier, *k* is the frequency component index, Δf is the interval between two frequency components , and N_s is the number of samples taken.

2.3.3 Envelope analysis

Envelope analysis, also known as the "High Frequency Resonance Technique", is based on analyzing the envelope signal obtained after filtering within a frequency range. The Hilbert Transform (HT), which provides the analytical representation of a real-valued signal, plays a crucial role in this technique [38]. The envelope of the signal *x(t)* is given by the following relation:

$$\hat{s}(t) = \frac{1}{\pi}\int_{-\infty}^{+\infty}\frac{s(\tau)}{t-\tau}d\tau \tag{2.13}$$

Where τ is a time variable.

The original signal *s(t)* and the signal $\tilde{s}(t)$ are added together to obtain the analytic signal $\hat{s}(t)$:

$$\hat{s}(t) = s(t) + j\tilde{s}(t) \tag{2.14}$$

The modulus of $\hat{s}(t)$ defines the envelope of *s(t)*, i.e., its demodulation:

$$|\hat{s}(t)| = \sqrt{s(t)^2 + \tilde{s}(t)^2} \tag{2.15}$$

The envelope technique using filtering is highly selective, as it takes into account the vibration mode with a sufficiently high signal-to-noise ratio. The choice of the filter's bandwidth must cover all the frequency components caused by the resonance frequency.

Building on the fundamental vibration analysis principles, the following section formalizes the mathematical representation of vibration signals to enable advanced deconvolution-based processing.

3 Mathematical modeling of vibration signals

The detection of mechanical faults in rotating machinery (particularly those affecting rolling element bearings) relies on the accurate interpretation of vibration signals collected from the system during operation. These signals result from the dynamic interaction between excitation sources (typically fault-induced impulsive events) and the transmission path through which these excitations are conveyed to the sensors. To enable systematic analysis and the application of advanced signal processing methods, it is essential to adopt a mathematical model that reflects this physical process.

$$s(t) = g(t) * u(t) + n(t) \tag{2.16}$$

Where * denotes convolution, *s(t)* is the measured vibration signal, *u(t)* is the source signal, *g(t)* is the impulse response of the transmission path, and *n(t)* represents additive noise.

3.1 Impulse response and excitation signal

The system response characterizes how an impulsive mechanical input is transmitted through the components of the machine; such as shafts, and bearings, before reaching the sensor. This response inherently filters the original signal and may introduce resonance phenomena or dispersion, depending on the structure’s characteristics.

The excitation, typically sparse in time, represents physical phenomena such as impacts caused by localized defects on bearing raceways. These excitations are often periodic or quasi-periodic, governed by the rotational speed and geometric properties of the bearing assembly. Detecting these sparse events is crucial for fault diagnosis, yet they are often masked by the system's dynamic filtering and the presence of noise.

3.2 Additive noise and measurement limitations

In practical diagnostic scenarios, the recorded signal is contaminated by noise, which can stem from a variety of sources: sensor electronics, structural vibrations unrelated to the fault, or environmental interferences. This noise may be stochastic or deterministic and typically reduces the signal-to-noise ratio, particularly in the early stages of defect development. In addition, measurement systems introduce further limitations, such as finite sampling rates, analog-to-digital quantization, limited sensor bandwidth, and positioning inaccuracies. These factors necessitate robust signal processing strategies capable of isolating fault-related components from a degraded or mixed signal.

Having established the convolutional nature of vibration signals, this section introduces the fundamental concepts of deconvolution and the associated mathematical difficulties.

4 Deconvolution in signal processing

4.1 Convolution/ Deconvolution process

4.1.1 Continuous domain representation

In the continuous-time domain, the observed vibration signal can be modeled as the convolution of an unknown excitation signal, representing impulsive fault activity, with the system's impulse response, which reflects the dynamic behavior of the mechanical structures (see Figure 2.2).

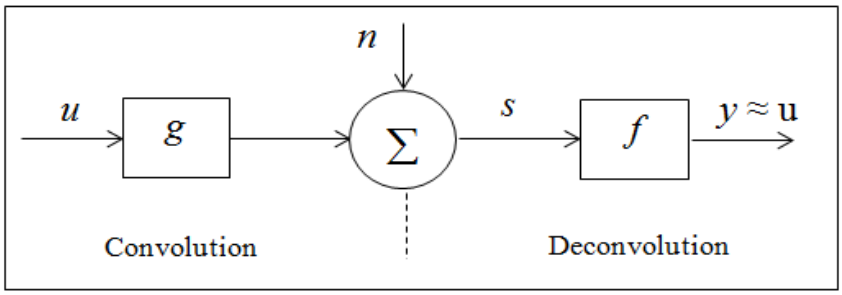

Figure 2.2: Convolution/deconvolution basic process

Case 1: Without noise:

$$s(t) = g(t) * u(t) = \int_{-\infty}^{+\infty} g(k)u(t-k)dk \quad (2.17)$$

Where * denotes convolution.

In the frequency domain, this convolution translates into a multiplication:

$$S(f) = G(f)\,.\,U(f) \;\leftrightarrow U(f) = \frac{S(f)}{G(f)} \quad (2.18)$$

Where $S(f)$, $G(f)$, and $U(f)$ represent the FT of $s(t)$, $g(t)$ and $u(t)$, respectively.

Case 2: With noise:

$$s(t) = (g * u)(t) + n(t) = \int_{-\infty}^{+\infty} g(k)u(t-k)dk + n(t) \quad (2.19)$$

Where $n(t)$ accounts for additive noise due to measurement imperfections and external disturbances. In the frequency domain, the Eq. (2.19) is defined as:

$$S(f) = G(f)\,.\,U(f) + N(f) \quad (2.20)$$

Where $N(f)$ is the spectral representation of the noise.

By dividing both sides of this equation by *G(f)*, we obtain:

$$\widetilde{U}(f) = U(f) + \frac{N(f)}{G(f)} \quad (2.21)$$

The estimated signal $\widetilde{U}(f)$ is obtained by simply dividing (2.21) by the system transfer function *g*. The last term shows that noise *N(f)* is strongly amplified wherever *G(f)* is small. As a result, $\tilde{u}(f)$ is often corrupted by oscillatory components and becomes practically unusable without stabilization techniques.

4.1.2 Discrete domain representation

In practical applications, signals are discretely sampled, leading to the discrete convolution formulation:

$$s[j] = \sum_{0}^{M-1} g[k]u[j-k] + n[j] \quad (2.22)$$

Or in matrix form, it is defined as:

$$s = Gu + n \quad (2.23)$$

Where:

- $s, u, n \in \mathbb{R}^N$, are vectors of the observed signal, the excitation, and the noise respectively,
- G $\in \mathbb{R}^{N\times N}$ is a convolution matrix,

The convolution matrix G $\in \mathbb{R}^{N\times N}$ is typically Toeplitz, meaning each diagonal from top-left to bottom-right is constant. This structure captures the finite-length, time-invariant nature of the system's response. However, Toeplitz matrices arising from impulse responses are often ill-conditioned, meaning that their smallest singular values are close to zero. As a result, inversion of G in the presence of noise leads to significant error amplification, particularly along the directions associated with these small singular components.

In the absence of noise, the inverse problem reduces to finding *u* such that:

$$Gu = s \tag{2.24}$$

The formal solution is:

$$u = G^{-1}s \tag{2.25}$$

However, this inversion is sensitive to the conditioning of G. The condition number:

$$\mathcal{C}(G) = \|G\| \,.\, \|G^{-1}\| = \sqrt{\frac{\gamma_{max}}{\gamma_{min}}} \tag{2.26}$$

Equation (2.26) indicates the stability of inversion. A high condition number implies ill-conditioning, leading to large errors in *u* when noise is present.

When noise corrupts the signal *s*, the solution becomes:

$$\tilde{u} = G^{-1}(s + n) = u + G^{-1}n \tag{2.27}$$

The noise *n* is thus amplified by G^{-1}, especially along directions corresponding to small singular values of G.

Therefore, deconvolution problems must be regularized to prevent instability and produce meaningful fault features. In what follows, we introduce the concept of ill-posed inverse problem, followed by various regularization techniques.

The discrete formulation of the deconvolution problem, as developed in the previous section, highlights the transformation of a convolution operation into a linear inverse problem involving structured matrices; most often Toeplitz or circulate. While this formulation allows for numerical implementation and paves the way for algorithmic solutions, it also exposes a critical challenge: the instability inherent in direct inversion. In practical scenarios, the presence of measurement noise, limited resolution, and the spectral overlap between the signal and the system response contribute to an unreliable recovery of the underlying excitation. This leads to a deeper mathematical concern known as ill-posed problem, where small perturbations in the observed

signal can cause disproportionately large deviations in the reconstructed source. The next section is therefore devoted to formally analyzing the ill-posed nature of deconvolution problems, through the lens of Hadamard's criteria, and to discussing its implications for vibration-based signal reconstruction.

4.2 Inversion and ill-posed nature

The key objective in this context is to recover the underlying excitation from the measured signal, which is viewed as the outcome of a convolution process involving an unknown or partially known system response. This leads to a classical inverse problem in signal processing:

Given *s(t)* and (possibly unknown) *g(t)*, estimate *u(t)* such that

$$s(t) \approx g(t) * u(t) + n(t) \tag{2.28}$$

By discretizing the model over a finite observation window with sampling step, we obtain:

$$s = Gu + n \tag{2.29}$$

Where:

- $s \in \mathbb{R}^N$ is the discrete measurement vector,
- G $\in \mathbb{R}^{N \times N}$ is the convolution matrix built from the system response $g(t)$,
- $u \in \mathbb{R}^N$ is the unknown vector representing the excitation or fault signature,
- $n \in \mathbb{R}^N$ captures measurement noise.

This constitutes a classical inverse problem: to recover *u* from noisy observations *s*, knowing or estimating G. In practical scenarios, G is often only partially known or estimated from experimental data, further increasing the challenge.

A minor fluctuation in a few entries of *s*, due to noise or measurement uncertainty, can induce large oscillations or distortions in the recovered signal *u*, as depicted in Figure 2.3.

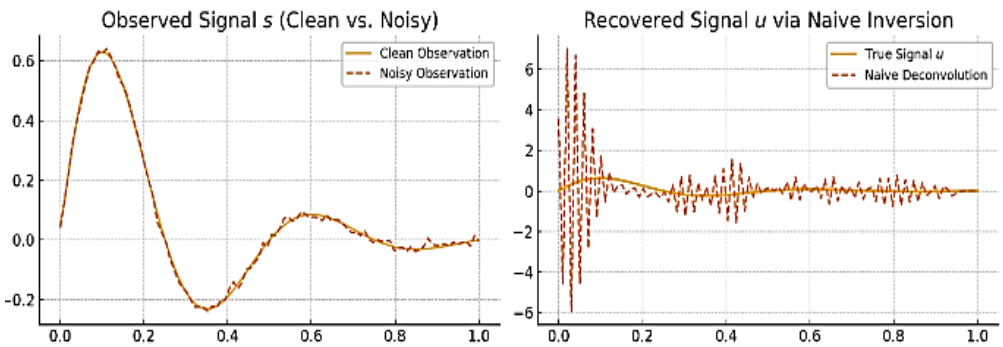

Figure 2.3: Illustration of noise amplification during naïve deconvolution

This figure demonstrates how a small amount of noise in the observed signal *s* can be dramatically amplified when attempting naive inversion using a pseudo-inverse of the convolution matrix G. The result is a highly unstable estimate of the true signal *u*, visually confirming the ill-posed deconvolution problem, particularly in terms of stability (one of Hadamard's criteria).

In theory, the inverse problem *s* provides a direct path to fault signal recovery. However, in practice, noise and ill-conditioning of G make this inversion unstable. This leads us to the broader class of ill-posed problems, as characterized by Hadamard.

4.3 Hadamard's criteria of well-posed nature

In his foundational work on boundary value problems, Hadamard [36] proposed that a well-posed mathematical model must satisfy three essential criteria:

- Existence: A solution should exist for the problem under investigation,
- Uniqueness: This solution must be the only one compatible with the given data,
- Stability: The solution should vary continuously with changes in the data; small errors or perturbations in the input should not produce large deviations in the output.

These principles are crucial in the diagnostic setting, where vibration measurements are inevitably affected by instrumental noise, environmental disturbances, and uncertainties in the system's dynamic response.

These three criteria below are essential to ensure a reliable and meaningful model for diagnosis:

- If no solution exists, then the model may be inadequate or the data insufficient,
- If multiple solutions exist, the system is underdetermined, indicating missing constraints or insufficient information about the structure or source of excitation,
- If the solution is unstable, then even minor noise in the recorded data can produce large errors in the recovered excitation, rendering the result practically useless.

Among these, stability is often the most critical concern in real-world applications. Since all measurements are subject to some level of error, any useful solution must be robust to such perturbations. A model that fails this condition (despite satisfying the other two) can yield misleading or non-physical results. If the model does not incorporate sufficient prior knowledge or constraints, no algorithmic adjustment can guarantee meaningful recovery of the true signal.

To mitigate the effects of an ill-posed problem, particularly in the presence of noise and incomplete system knowledge, one must incorporate regularization techniques. These methods aim to stabilize the solution by embedding additional information (such as smoothness, sparsity, or entropy criteria) into the inversion process.

The inverse problem consists of recovering u from the observation s. This inverse problem is said to be well-posed in the sense of Hadamard if the following three conditions are satisfied:

1. **Existence:** For every $s \in H_2$, there exists at least one $u \in H_1$ such that:
$$\mathcal{G}(u) = s \tag{2.30}$$
2. **Uniqueness:** For every $s \in H_2$, there is at most one $u \in H_1$ satisfying:
$$\mathcal{G}(u) = s \tag{2.31}$$
3. **Stability:** The solution u depends continuously on the data s. That is, for any sequence $u_n \subset H_1$ such that for $(n \to \infty)$:
$$\mathcal{G}(u_n) \to \mathcal{G}(u) \text{ in } H_2 \tag{2.32}$$

It follows that:

$$u_n \to u \quad \text{in } H_1 \tag{2.33}$$

In deconvolution-based signal recovery, the inverse problem is often ill-posed in the Hadamard sense (existence, uniqueness, or stability) especially when the system response is poorly known or the signal is noisy. This ambiguity allows multiple plausible solutions, complicating the identification of true fault signatures. To address this, advanced methods like MED, Variational Mode Decomposition (VMD), and Blind Separation Sources (BSS) have been developed [54, 71], though they may struggle with restoring sparse impulsive features. Regularization techniques are thus essential to stabilize solutions and enhance diagnostic relevance. Because direct inversion of the convolution process is often unstable, it becomes necessary to introduce regularization strategies, which are discussed below.

5 Regularization strategy

As discussed earlier, the deconvolution of vibration signals from the machine–converter system is a typical example of an ill-posed inverse problem. The main challenge is the instability and non-uniqueness of the solution when attempting to recover the unknown excitation (fault) signal from the observed signal. To overcome the instability of this inverse problem, it is necessary to introduce additional criteria that enable the selection of a physically meaningful

solution among the many mathematically possible ones. This process, known as regularization, incorporates prior information about the expected properties of the solution, such as its smoothness or frequency content, combined with the data fidelity criterion based on the closeness of the reconstructed excitation $\tilde{u}$ to the measured signal s.

Regularization is particularly important in situations where the number of unknowns exceeds the number of measurements, leading to an underdetermined system with infinitely many solutions. By regularizing the problem, we accept that the true fault signal cannot be perfectly recovered from noisy measurements alone. Instead, knowledge about the system's impulse response.

Instead, the system's impulse response g, used as prior information, defines a class of admissible solutions g defines a class of admissible solutions, among which some are physically relevant while others are artifacts of noise or mathematical ambiguity.

The choice of a regularization strategy introduces a controlled degree of freedom in the reconstruction process, steering the solution toward specific desired properties in the estimated signal $\tilde{u}$. This principle of 'solution selection' highlights that the regularized estimate is inherently non-unique and constitutes merely one admissible solution among the set of all possibilities compatible with the measured data and the imposed prior information.

5.1 Philosophy of regularization

We define two distance measures to formalize the concept of regularization:

- $L_1(\tilde{u}, \tilde{u}_0)$: Distance between the estimated solution $\tilde{u}$ and an ultra-rough solution $\tilde{u}_0$, usually obtained by a least-squares criterion,
- $L_2(\tilde{u}, \tilde{u}_\infty)$: Distance between $\tilde{u}$ and an ultra-smooth solution $\tilde{u}_\infty$.

The regularized solution $\tilde{u}(\alpha, s)$ is then defined as the minimizer of the composite criterion:

$$L\{\tilde{u}(\alpha, s)\} = L_1(\tilde{u}, \tilde{u}_0) + \alpha L_2(\tilde{u}, \tilde{u}_\infty) \qquad with \qquad \tilde{u} \in \mathcal{U} \tag{2.34}$$

Where $\mathcal{U}$ denotes the set of all mathematically admissible solutions, and $\alpha \geq 0$ is the regularization parameter controlling the trade-off between fidelity to the data and adherence to the prior.

- For $\alpha = 0$, the solution reduces to the least-squares estimator $\tilde{u}_0$, appropriate when the data highly reliable.

- As $\alpha \to +\infty$, the solution tends to the ultra-smooth solution $\tilde{u}_\infty$, relying mainly on prior assumptions and ignoring the data.

The purpose of regularization is to find a balanced compromise by selecting an optimal α minimizing the criterion L.

5.2 Various regularization approaches

5.2.1 Zero-order or minimal norm regularization

When the solution amplitude is known to be bounded, this information can be encoded by minimizing the norm of the solution:

$$L_2(\tilde{u}, \tilde{u}_\infty) = \|\tilde{u}\|_2^2 = \sum_{k=0}^{N-1} \tilde{u}_k^2 \tag{2.35}$$

and using a least-squares criterion for L_1 :

$$L_1 = \|s - G\tilde{u}\|_2^2 \tag{2.36}$$

The combined regularization criterion becomes:

$$L = \|s - G\tilde{u}\|_2^2 + \alpha\|\tilde{u}\|_2^2 \tag{2.37}$$

This simple approach penalizes solutions with excessively large amplitudes.

5.2.2 Tikhonov-Miller regularization

Tikhonov regularization generalizes the zero-order approach by incorporating a constraint operator D, chosen to promote specific solution characteristics (e.g., smoothness):

$$L = \|s - G\tilde{u}\|_2^2 + \alpha\|\tilde{u}\|_2^2 \tag{2.38}$$

Where D is typically a discrete derivative operator, such as:

- Gradient: $D = [1, -1]$,
- Laplacian: $D = [-1, 2, -1]$.

The solution is obtained by solving:

$$(G^T G + \alpha\, D^T D)\tilde{u} = G^T s \Longrightarrow \tilde{u} = (G^T G + \alpha D^T D)^{-1} G^T s \tag{2.39}$$

The generalized matrix $G^+ = G^T G + \alpha\, D^T D$ is better conditioned than $G^T G$ alone, improving numerical stability by effectively filtering out components associated with small eigenvalues that cause instability.

The conditioning of this matrix is characterized by the ratio:

$$C(G^{+}) = \frac{\max(\lambda_G + \alpha\lambda_D)}{\min(\lambda_G + \alpha\lambda_D)} \tag{2.40}$$

Where λ_G and λ_D are eigenvalues of $G^T G$ and $D^T D$, respectively. The matrix G^{+}must preserve the large eigenvalues of $G^T G$ and replace the small ones (which are the source of instability) with those of $\alpha D^T D$, Thus, since H is a low-pass filter, D must be a high-pass filter.

The choice of the regularization parameter α is crucial: it balances noise suppression and signal fidelity but is difficult to estimate precisely.

5.3 Regularization parameter α choice and impact

The regularization parameter α plays a pivotal role in the outcome of the inversion. A small value may lead to solutions that are highly sensitive to noise, while a large α may oversmooth the signal and obscure fault-related features. In the literature, several techniques have been proposed to guide the choice of α including the L-curve method, generalized cross-validation (GCV), and the discrepancy principle [37, 76]. However, in practical applications, particularly in vibration-based fault diagnosis such methods may not always yield satisfactory or interpretable results due to non-Gaussian noise or complex signal structures. In this work, the value of α is selected empirically through careful adjustment, based on a compromise between residual energy and the clarity of the extracted fault-related components. This empirical tuning, guided by physical intuition and diagnostic objectives, proves effective in stabilizing the inversion without suppressing the informative content of the signal [37].

The instability encountered in deconvolution problems can be understood through the singular value decomposition (SVD) of the convolution matrix G. The SVD reveals that G can be expressed as:

$$G = U\Sigma V^T, \qquad \Sigma = \mathrm{diag}(\sigma_1, \sigma_2, \ldots, \sigma_N)$$

Where $\sigma_1 \geq \sigma_2 \geq \ldots \sigma_N \geq 0$ are the singular values. In vibration signals from machine-converter systems, many singular values are very small or decay rapidly to zero. These small singular values correspond to high-frequency components in the solution space that are highly sensitive to noise. During direct inversion, noise is amplified by terms proportional to $1/\sigma_i$, leading to unstable and oscillatory solutions; a direct manifestation of the ill-posed nature of the problem.

Tikhonov–Miller regularization addresses this instability by effectively filtering the singular values, yielding a stable and physically meaningful estimate. The regularization parameter α controls this damping, balancing noise suppression against solution fidelity.

6 Deconvolution methods

Signal processing often relies on mathematical models that relate measurable data (such as vibration signals) to physical causes, including impulsive forces generated by defects. The investigation of restoring original signals from measured data has attracted significant attention in recent research, in which various restoration techniques were developed; such as: wavelet transform [56],[44], VMD [27],[55], Empirical Mode Decomposition (EMD) [39],[48], BSS [40],[71] and the MED [6,54,57,81] etc. They have been widely adopted for non-stationary signal analysis; unfortunately, they often fall short in accurately restoring the temporal sparsity of impulsive fault signatures, especially when these are strongly masked by system dynamics.

More recently, blind deconvolution approaches have received growing attention due to their ability to reverse the convolutional effects of the transfer path and directly enhance impulsive features indicative of defects [57], [44]. Nevertheless, blind deconvolution remains an ill-posed inverse problem, often requiring additional constraints to ensure meaningful solutions.

Recent studies; such as those presented in [59, 4, 14, and24] have demonstrated the effectiveness of combining regularization frameworks with multiresolution or sparsity-based techniques to improve the deconvolution performance in both theoretical and applied domains. The task of ill-posed nature (in the sense introduced by Jacques Hadamard) of inverse problems leads to the use of regularization or adaptive deconvolution techniques to obtain a meaningful solution [36].

In this context, the present study proposes a hybrid deconvolution strategy that combines MED with the VC algorithm to effectively recover fault-related signals embedded in noisy vibration measurements.

Before introducing the combined approach, we briefly review several decomposition techniques commonly used in bearing fault diagnosis. Among these methods, Minimum Entropy Deconvolution (MED) stands out because of its remarkable capacity to enhance impulsive components that are otherwise obscured by noise, structural resonances, and broadband machine

dynamics. Its primary strength lies in maximizing the non-Gaussianity of the reconstructed signal, which directly emphasizes sparse, transient events characteristic of bearing defects.

To achieve this, MED determines a set of filter coefficients that, when applied to the measured signal, amplify the underlying impulsive structure. In practice, this amounts to constructing an FIR filter that not only mitigates convolution effects but also drives the output toward a sequence of sharp transients. As a result, MED provides a significantly clearer preliminary extraction of fault-induced impulses.

However, while MED excels at revealing impulsive content, its ability to fully recover the original excitation remains limited. Residual smearing or distortion may persist, particularly when the system response is strongly blurred or the signal-to-noise ratio is low. To address this limitation, the Tikhonov-regularized VC algorithm is introduced as a second step, refining the reconstruction through an iterative deconvolution process.

The following sections present the theoretical and algorithmic basis of MED and the Van Cittert method in detail.

7 Minimum entropy deconvolution

MED was initially introduced by Wiggins in 1978 in the field of seismic signal processing [82], with the aim of enhancing reflection events by recovering sparse reflectivity sequences. The main idea is to design a linear filter that maximizes the non-Gaussianity of the output signal, using kurtosis as a measure of impulsiveness. Mathematically, this optimization process converges to a filter that approximates the inverse of the system's impulse response.

This method was subsequently adopted in mechanical fault diagnosis, proving particularly effective for detecting localized defects in rolling element bearings [58]. In this context, the primary objective of the MED algorithm is to design a finite impulse response (FIR) filter that counteracts the smearing effect of the vibration transmission path. It achieves this by maximizing the kurtosis of the output signal to enhance the fault transients. Thus, the process of enhancing impulsive features implicitly computes an estimate of the inverse system response between the fault and the sensor.

Novel research has robustly demonstrated that MED is highly effective for extracting repetitive impulsive features masked by structural resonances and noise in vibration signals [58, 68]. These studies established MED as a powerful preprocessing step for techniques such as

envelope analysis, resonance demodulation, and cyclostationary analysis. Today, MED is widely integrated with other signal processing tools, including spectral kurtosis and adaptive filtering. More recently, its role as a blind system identifier has made it a key component in hybrid frameworks, where it is used in conjunction with iterative deconvolution algorithms and blind source separation methods, solidifying its place in automated bearing fault detection pipelines [53, 58].

7.1 Mathematical model and signal representation

In the context of fault diagnosis of localized defects (such as bearing faults), the measured vibration signal is modeled as the output of a linear system as follows:

$$s[j] = (g * u)[j] + n[j] = \sum_{k=0}^{M-1} g[k]u[j-k] + n[j] \quad (2.41)$$

where:

- $u[j]$ is the original excitation signal, assumed impulsive, i.e., a sequence of short, rare events typical of localized faults.
- $g[k]$ is the system's impulse response (the vibration transmission path between the defect and the sensor), which modulates and spreads these impulses.
- $n[j]$ is additive noise (often modeled as white or colored noise).
- M is the effective length of the impulse response

The primary objective of MED in this framework is to estimate the inverse filter $f[k] \approx g^{-1}[k]$ that reverses the convolutional effect of the system.

7.2 Filter and filtered signal

We seek a Finite Impulse Response (FIR) filter that acts as an inverse filter for the system.

$$f = [f[0], f[1], \dots, f[L-1]] \quad (2.42)$$

of length L, such that when applied to the measured signal s[j], it produces an output that approximates the original excitation:

$$y[j] = \sum_{k=0}^{L-1} f[k]s[j-k] \approx u[j] \quad (2.43)$$

The critical mathematical relationship emerges from the convolution process:

$$y[j] = f[j] * s[j] = f[j] * (g[j] * u[j]) = (f[j] * g[j]) * u[j] \quad (2.44)$$

For y[j] to approximate u[j], the composite filter must satisfy:

$$f[j] * g[j] \approx \delta[j] \quad (2.45)$$

Where $\delta[j]$ is the unit impulse function. This implies that $f[j]$ approximates the inverse system response: $f[j] \approx g^{-1}[j]$.

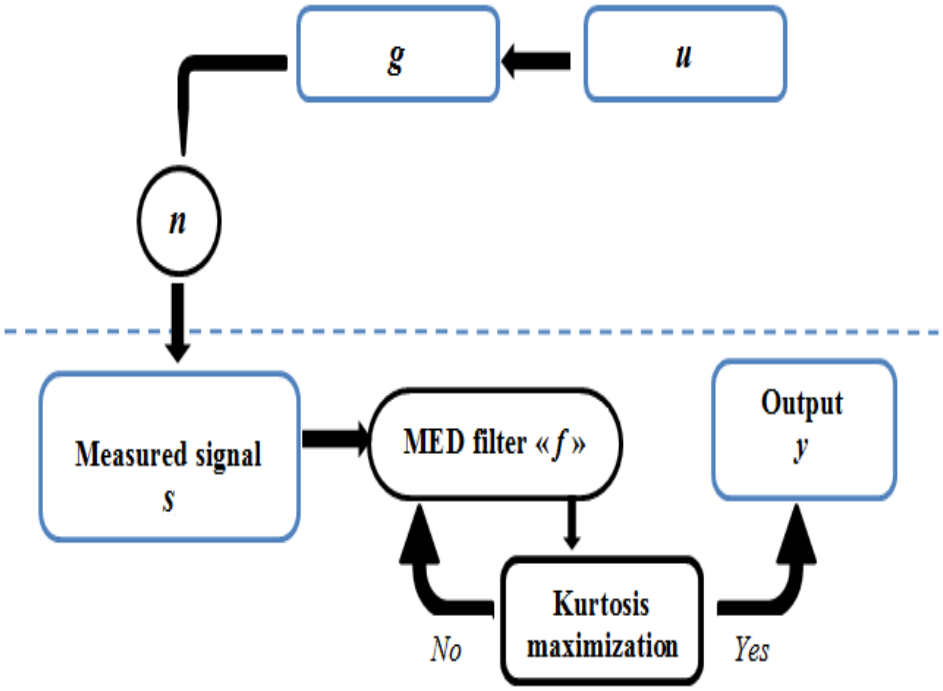

Figure 2.4: MED process

Figure 2.4 illustrates the fundamental process of MED, which aims to compute the optimal set of filter coefficients by maximizing the kurtosis of the output signal y(j).

7.3 Entropy minimization criterion (via kurtosis)

Direct minimization of Shannon entropy [40] of the discrete finite-length signal $y[j]$ is difficult. Wiggins (1978) [82] proposed to use kurtosis as a proxy for entropy because:

- Kurtosis measures the peakedness or impulsiveness of a signal,

- Signals with rare impulsive peaks exhibit high kurtosis (values concentrated around zero with few extreme values),
- Gaussian signals (like noise) have zero kurtosis (centered at zero after subtracting 3).

Formally, the kurtosis K of $y[j]$ is defined as:

$$K = \frac{E[y[j]^4]}{(E[y[j]^2])^2} - 3 \tag{2.46}$$

with $$y = fs + n \tag{2.47}$$

Where $E[\cdot]$ represents the expectation operator.

7.4 Matrix formulation of the problem

For numerical implementation, we construct the Toeplitz matrix $S \in \mathbb{R}^{N \times L}$ from the measured signal s[j] as:

$$S = \begin{bmatrix} s[0] & 0 & \cdots & 0 \\ s[1] & s[0] & \cdots & 0 \\ \vdots & \vdots & \ddots & \vdots \\ s[N-1] & s[N-2] & \cdots & s[N-L] \end{bmatrix} \tag{2.48}$$

Then the filtered output can then be written as a matrix-vector product:

$$Y = Sf \tag{2.49}$$

Where

$$f = [f[0], f[1], \ldots, f[L-1]]^T \in \mathbb{R}^L \tag{2.50}$$

7.5 The objective function

The core optimization problem in MED is formulated as the maximization of output kurtosis to estimate the inverse filter *f*. The corresponding objective function is defined as:

$$J(f) = \frac{\sum_{j=1}^{N} y[j]^4}{\left(\sum_{j=1}^{N} y[j]^2\right)^2} = \frac{\sum_{j=1}^{N} y[j]^4}{(y^T y)^2} \tag{2.51}$$

This optimization is carried out over all filters satisfying the unit-norm condition

$$\|f\|_2 = 1 \tag{2.52}$$

This normalization prevents degenerate solutions and ensures numerical stability. The objective function J*(f)* selects filter coefficients that amplify impulsive peaks, which mathematically corresponds at least approximately to constructing a filter satisfying $f = g^{-1}$.

7.6 Nonlinear and iterative optimization problem

The maximization of the kurtosis objective function leads to a nonlinear and non-convex optimization problem, formally expressed as:

$$\max_{f \subset \mathbb{R}^L, \|f\|_2 = 1} \mathrm{J}(f) \tag{2.53}$$

This is a non-convex, nonlinear problem requiring iterative algorithms, such as:

- Gradient-based methods on $\mathrm{J}(f)$,
- Fixed-point algorithms based,
- Modified Newton methods based on Hessian approximations [54, 59],
- Algorithms based on local maximization of kurtosis.

7.7 Filter coefficients estimation

The MED algorithm computes the FIR filter coefficients through an iterative estimation process. The coefficients are updated at each iteration using the following formula:

$$f_{m,l} = \frac{E[y_m(k) s_{en}(k-l)]}{E[(s_{en}(k-l))^2]} \quad \text{for } l = 0, \dots, L-1 \tag{2.54}$$

Where $f_{m,l}$ represents the filter coefficient at iteration *m*, $y_m(k)$ denotes the filtered output signal and $s_{en}(k-l)$ is a normalized version of the input signal.

This process continues until convergence, producing a final filter that, when applied to the vibration signal, yields a deconvolved output with enhanced fault impulses.

Demonstration:

Consider the mean squared error function:

$$J(f_{m,l}) = E\left[\left(y_m(k) - f_{m,l} s_{en}(k-l)\right)^2\right] \tag{2.55}$$

Where $J(f_{m,l})$ represents the mean squared error.

Setting the partial derivative with respect to $f_{m,l}$ equal to zero:

$$\frac{\partial E}{\partial f_{m,l}} = -2E[y_m(k) s_{en}(k-l)] + 2 f_{m,l} E[(s_{en}(k-l))^2] = 0 \tag{2.56}$$

Solving equation (2.56) yields the optimal coefficient estimate:

$$f_{m,l} = \frac{E[y_m(k)s_{en}(k-l)]}{E[(s_{en}(k-l))^2]} \tag{2.57}$$

This relation shows that each filter coefficient is the best linear least squares estimate relating the filtered output and the delayed input signal.

8 Van Cittert algorithm: principle and regularization

The VC algorithm is a classical iterative method for solving the inverse problem associated with convolution equations, particularly when aiming to retrieve the unknown excitation or fault signature from a blurred or noisy observation. Originally introduced by Van Cittert in 1931 [79], this algorithm remains foundational due to its conceptual simplicity and extensibility.

Let us consider the discrete convolution model:

$$s = \mathrm{G}u + n \tag{2.58}$$

Where:

- $\mathrm{s} \in \mathbb{R}^N$ is the discrete measurement vector,
- $\mathrm{G} \in \mathbb{R}^{N\times N}$ is the convolution matrix built from the system response $g(t)$,
- $u \in \mathbb{R}^N$ is the unknown vector representing the excitation or fault signature,
- $n \in \mathbb{R}^N$ captures measurement noise.

The objective is to recover *u* from the noisy observation *s*, which poses an inverse problem. In the absence of noise, the problem reduces to solving the linear system $s = Gu + n$. However, direct inversion is often ill-posed or unstable in practice.

8.1 Iterative scheme

The Van Cittert algorithm proposes an iterative reconstruction of *u* through the following recursive relation:

$$\begin{cases} u^{(0)} = s, \\ u^{(k+1)} = u^{(k)} + \left(s - \mathrm{G}u^{(k)}\right) \end{cases} \tag{2.59}$$

At each iteration k, the current estimate $u^{(k)}$ is updated by adding the residual $r^{(k)} = s - \mathrm{G}u^{(k)}$, which reflects the mismatch between the measured signal and the one reconstructed by convolution. This residual is interpreted as a correction term driving the solution toward

convergence. Assuming G is non-singular and the system is noise-free, the iterative process converges to:

$$u^{(\infty)} = G^{-1}s \tag{2.60}$$

Which is equivalent to the classical inverse filtered solution. However, in practical applications where noise is present, this naive formulation can lead to instabilities and divergence, especially as high-frequency noise components are successively amplified.

8.1.1 Regularized formulation (Miller regularization)

To address the ill-posed nature and sensitivity to noise, regularization is introduced into the VC framework. Specifically, Miller regularization [76] modifies the inversion process by penalizing undesired oscillations in the estimated solution.

Let $\mathrm{D} \in \mathbb{R}^{N\times N}$ denote a discrete differential operator, and $\alpha > 0$ a regularization parameter. The regularized convolution operator is then defined as:

$$\mathrm{G}^{+} = \mathrm{G}^{T}\mathrm{G} + \alpha \mathrm{D}^{T}\mathrm{D} \tag{2.61}$$

Replacing the iterative resolution of $s = Gu$ with that of $\mathrm{G}^{T}s = (\mathrm{G}^{T}\mathrm{G} + \alpha \mathrm{D}^{T}\mathrm{D})u$. The regularized VC algorithm is formulated as:

$$\begin{cases} u^{(0)} = s, \\ u^{(k+1)} = u^{(k)} + (\mathrm{G}^{T}s - (\mathrm{G}^{T}\mathrm{G} + \alpha \mathrm{D}^{T}\mathrm{D})u^{(k)}) \end{cases} \tag{2.62}$$

This formulation stabilizes the inversion by incorporating a priori knowledge about the desired smoothness or sparsity of u, and prevents the amplification of noise. The regularization term $\alpha \mathrm{D}^{T}\mathrm{D}u^{(k)}$ acts as a smoothing constraint, prevent sudden changes in the estimated signal.

8.1.2 Practical relevance

VC algorithm, particularly in its regularized form, is well-suited for vibration-based fault diagnosis where the observed signal *s* results from the convolution of an impulsive excitation *u* (e.g., due to a bearing defect) with the system response *g(t)*. Regularization enables the algorithm to recover subtle impulsive features buried in noise, thus enhancing fault detection performance.

Building on the theoretical developments of the previous sections, the proposed hybrid deconvolution framework combines both MED and the regularized VC algorithm to achieve robust and interpretable signal reconstruction.

9 Proposed procedure

This work introduces a novel deconvolution framework aimed at effectively extracting periodic impulse signatures related to bearing faults from measured vibration signals. The vibration signal captured by an accelerometer is considered to be a convolution of the underlying impulsive excitation with the system's transmission path, contaminated by noise. Recovering the original impulses constitutes an ill-posed inverse problem that cannot be adequately addressed by direct inversion techniques due to instability and noise sensitivity.

To overcome these challenges, we propose an hybrid deconvolution method that combines MED and a regularized VC algorithm. This approach exploits the ability of MED to adaptively adjust the filter coefficients and the stability of the VC scheme in recovering the true excitation signal using an a priori model and regularization.

Step 1: Initial deconvolution using MED

The first step involves applying the MED algorithm to compute an adaptive FIR filter that maximizes the kurtosis of the deconvolved output. The principle of MED is to design a FIR filter that, when applied to the measured signal, produces an output signal with maximal impulsiveness; corresponding to a higher probability of fault-related features.

Let us consider the discrete convolution model described by the equation (2.58). MED identifies a filter f that maximizes the kurtosis of the filtered signal $y = f^T s$, yielding a deconvolved estimate that accentuates fault impulses. The optimal filter coefficients are approximated empirically using the relation presented in (2.54).

While MED is designed to maximize the impulsiveness of the measured vibration signal by enhancing kurtosis, its primary function is to estimate an inverse filter that amplifies impulsive features in the data. However, MED does not explicitly solve the underlying convolutional inverse problem between the original fault excitation u and the transmission path G. The measured vibration signal results from the convolution s = G*u + n, and while MED finds a filter that enhances impulsiveness, it does not guarantee a precise inversion of G to recover u directly. Because the transmission path typically acts as a smoothing or dispersive filter, recovering u from s constitutes an ill-posed inverse problem where direct inversion is unstable and sensitive to noise. Although MED effectively increases impulsive content to support fault detection, it cannot fully restore the original fault signature. Therefore, an additional iterative deconvolution step

such as the regularized Van Cittert algorithm; is necessary to solve the inverse convolution problem in a stable and reliable manner.

Step 2: Applying regularized VC algorithm

To overcome the limitations of the initial estimate, the second step applies the VC algorithm with Tikhonov-Miller regularization. This method progressively refines the deconvolution result by iteratively minimizing the discrepancy between the measured and reconstructed signals while stabilizing the solution through regularization. The initial condition $u^{(0)} = f^T s$ is typically set using the output of the MED-filtered signal, providing a strong impulsive structure to initialize the iterations.

The regularized VC algorithm is without imposed constraints, relying solely on the a priori assumption that the solution u is sufficiently smooth. The regularization term $\alpha D^\top D u^{(k)}$ suppresses high-frequency noise amplification and mitigates the instability caused by the ill-posed problem of the inversion.

To practically implement the proposed hybrid deconvolution strategy, the method is summarized in the following algorithmic form. The process starts with an impulsiveness-maximizing filter obtained through MED, followed by a refinement stage using a regularized VC scheme, ensuring both robustness and fidelity to the convolutional model.

❖ Algorithmic description of the proposed deconvolution method

Input: Measured signal $s \in \mathbb{R}^N$ (acquired from vibration sensor).

Output: Estimated excitation signal $\hat{u} \in \mathbb{R}^N$.

Step 1: MED

1. Initialize filter $f^{(0)} \in \mathbb{R}^M$ (e.g., random or unit impulse),
2. Define objective: maximize the kurtosis of the filtered signal $y(k) = f^T s(k)$,
3. Apply iterative update to maximize:

$$\mathrm{Kurt}(y) = \frac{\mathbb{E}[y^4]}{(\mathbb{E}[y^2])^2} \tag{2.63}$$

4. At convergence, obtain optimal deconvolution filter f_l .
5. Compute the deconvolved signal:

$$y = (f_l)^T s \tag{2.64}$$

The filtered output y serves as an initial impulsive estimate of the excitation.

Step 2: Regularized VC algorithm

6. Construct the convolution matrix $G \in \mathbb{R}^{N\times N}$ from system's estimated impulse response,
7. Define regularization matrix $D \in \mathbb{R}^{N\times N}$ (e.g., 1^{st} or 2^{nd} difference operator),
8. Initialize the excitation estimate with MED output:

$$u^{(0)} = y = (f_l)^T s \tag{2.65}$$

9. Choose regularization parameter $\alpha > 0$ and relaxation step $\mu > 0$.
10. For $k = 0,1, \dots, K_{\max}$
    a. Compute residual:

$$r^{(k)} = s - Gu^{(k)} \tag{2.66}$$

    b. Update estimate using VC scheme with Tikhonov-Miller regularization:

$$u^{(k+1)} = u^{(k)} + \mu\left(G^T r^{(k)} - \alpha D^T D u^{(k)}\right) \tag{2.67}$$

11. Repeat until convergence (e.g., $\left\|u^{(k+1)} - u^{(k)}\right\| < \epsilon$) 0,
12. Final estimate $\hat{u} = u^{(k)}$.

This integration of MED and VC create a complementary mechanism. First, MED is applied to estimate an inverse filter. Then, the VC iterative deconvolution algorithm is used to enforce the convolutional relationship and restore the original impulsive signal with improved stability. The detailed procedure of this method is illustrated in the following figure.

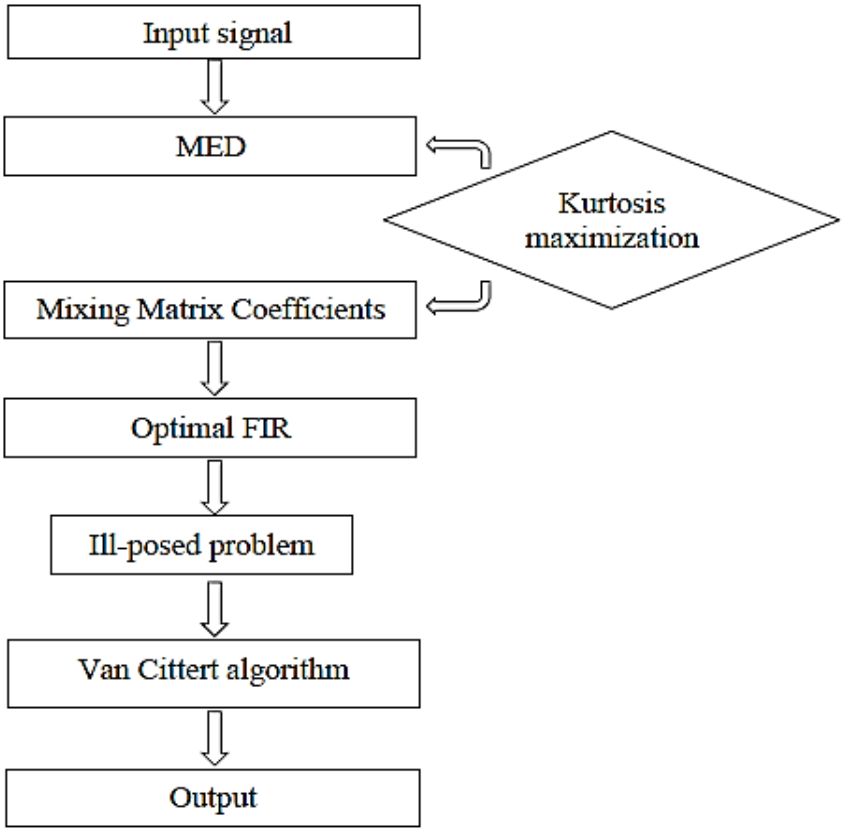

Figure 2.5: The flowchart of the proposed method

10 Conclusion

This chapter has presented the theoretical and methodological framework of the proposed deconvolution-based strategy for bearing vibration signal analysis. Starting from the mathematical modeling of vibration signals as convolution systems, the chapter addressed the ill-posed nature of the associated inverse problem and introduced regularization strategies to stabilize the inversion process. Among the deconvolution techniques reviewed, the MED and the VC algorithm were identified as powerful and complementary tools: MED determine filter coefficients, while the regularized VC algorithm refines the recovered signal by enforcing the convolutional consistency under stability constraints.

The combination of these two approaches yields a robust and efficient diagnostic strategy capable of revealing weak or obscured fault signatures in noisy environments. The next chapter will focus on the implementation of this hybrid method and its experimental validation on real bearing vibration data.

Chapter 3: Application of the proposed strategy for monitoring the operation state of bearings

1 Introduction

In this chapter, we present the application of the proposed method for bearing fault diagnosis. We begin with a description of the experimental setup used in the study. Subsequently, the application of the proposed combination of MED and VC is demonstrated on both simulated and real vibration signals collected from healthy and faulty bearings, including defects on the outer race, ball, and inner race. This approach enables the restoration of the original signal, leading to a more precise and reliable fault diagnosis.

2 Simulation study

In this section, a numerical simulation is conducted to assess the performance and relevance of the proposed two-stage methodology. To emulate the dynamic response of a defective bearing system, a synthetic signal is constructed to replicate the excitation caused by periodic impacts. Each impact is shaped by the superposition of two harmonic components and subject to exponential attenuation, thereby modeling the behavior of a modulated impulse response typical of rolling element bearing systems. The simulated signal is mathematically defined as follows:

$$x(t) = e^{-\varepsilon\tau}[\sin(2\pi f_1 t) + 3\sin(2\pi f_2 t)] \tag{3.1}$$

where

ε: a decay coefficient (not a frequency),

$\tau = mod(t_0, 1/fd)$: Time modulo operation used to reset the decay at each fault period.

f_1 and f_2 : resonance frequencies,

f_d : modulation or defect impact frequency,

$\tau = mod(t_0, 1/fd)$: Time modulo operation used to reset the decay at each fault period.

The simulated signal constructed in this study is intended to replicate the dynamic vibration response of a rolling element bearing with a localized defect. Such defects generate periodic impacts as rolling elements pass over them, exciting the structural resonances of the surrounding

system see Figure 3.1a. Each impact in the simulation is modeled as an impulsive signal composed of two harmonic components at different frequencies: f_1=2000 Hz and f_2=7000 Hz, with the second component weighted three times more than the first. This superposition introduces spectral asymmetry and complexity, which are typical features of real-world fault signals.

The amplitude envelope of each impulse follows an exponential decay, governed by the decay coefficient ε=800, which simulates the damping effect of the mechanical structure. This decay resets at regular intervals, enforced by a time modulation operation τ where the defect repetition frequency is 100Hz. This ensures that each impulse is regenerated periodically, simulating the passage of a defect at a consistent rate.

The signal is built by repeating individual impulse segments of duration T=0.01 s, sampled at a frequency of 12000 Hz, which corresponds to 120 samples per segment. These segments are concatenated to form a complete signal of N=4096 samples, with a total duration of approximately 0.3413 seconds for each signal.

To simulate a realistic operating environment, the original signal is contaminated with additive white Gaussian noise using an SNR of –0.5 dB, resulting in a noisy signal that presents a significant challenge for fault detection (see Figure 3.1b)). This simulated signal thus combines key elements observed in real-world bearing fault scenarios, including impulsiveness, modulation at the fault frequency, resonance excitation, damping, and background noise. It serves as an effective signature for evaluating the robustness and resolution of advanced signal processing techniques.

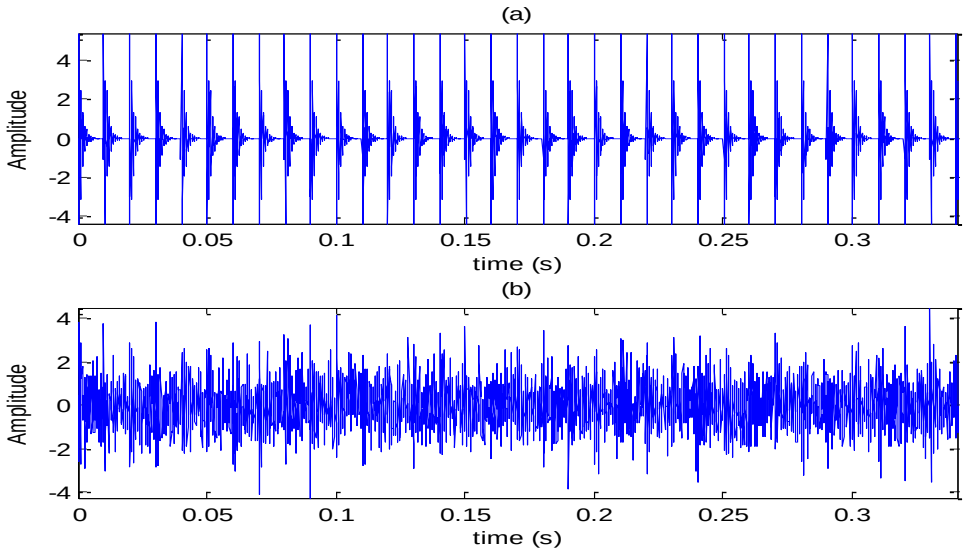

Figure 3.1: a) Simulated signal without noise, and b) Signal with noise

The simulated vibration signal, generated from Equation (3.1), is illustrated in Figure 3.1a with additive Gaussian noise, and in Figure 3.1b in its noise-free form. A comparison of the two signals reveals that periodic impulsive components are hardly noticeable in the noisy case, underscoring the challenge of time-domain analysis under low SNR conditions. The proposed methodology effectively addresses this issue by enhancing periodic structures within the signal, enabling the extraction of diagnostically relevant features.

In the first stage, the inverse filter is constructed using the MED technique. This filter, shown in Figure 3.2a, is iteratively optimized through kurtosis maximization, as illustrated in Figure 3.2b. Subsequently, the VC iterative algorithm is applied to further suppress residual noise while preserving impulsive structures. The resulting signal, presented in Figure 3.3, shows significantly clearer impulsive events, with a kurtosis of 3.96 compared to 3.67 for the original noisy signal, indicating enhanced impulsiveness and effective denoising.

When applied to the time-domain signal in Figure 3.1, the full reconstruction displayed in Figure 3.3 demonstrates the effectiveness of the proposed hybrid deconvolution strategy. The number, timing, and amplitude of impulsive events are accurately preserved, while residual noise is substantially reduced. These results, together with the kurtosis improvement, confirm the method's robustness in stationary additive noise environments. For deployment under more complex noise conditions or in safety-critical applications, further testing is recommended.

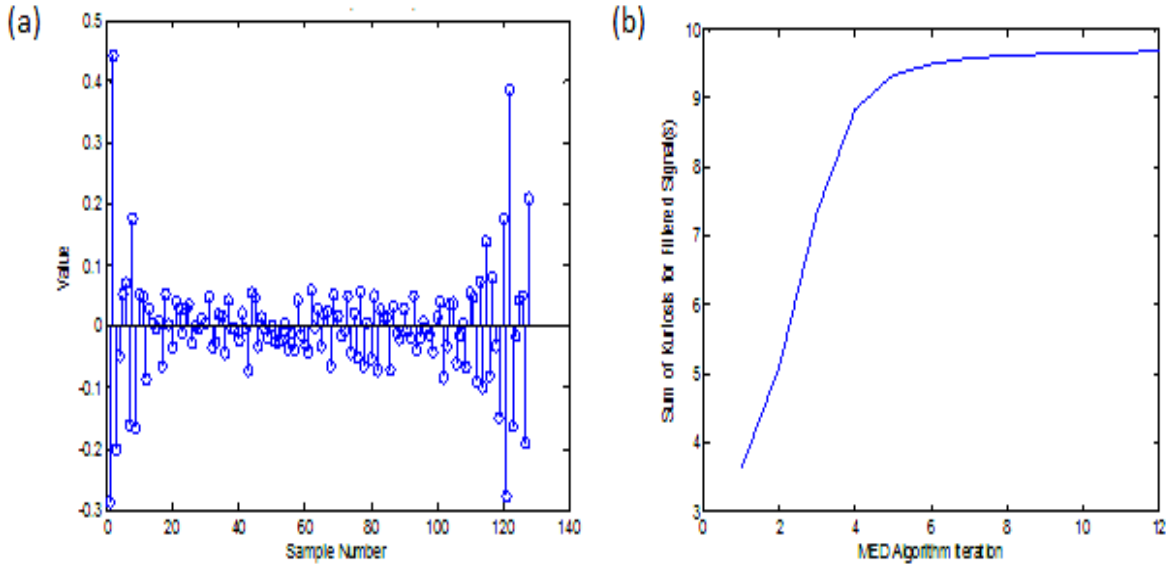

Figure 3.2: a) Final filter (FIR), and b) Maximization of kurtosis during MED algorithm

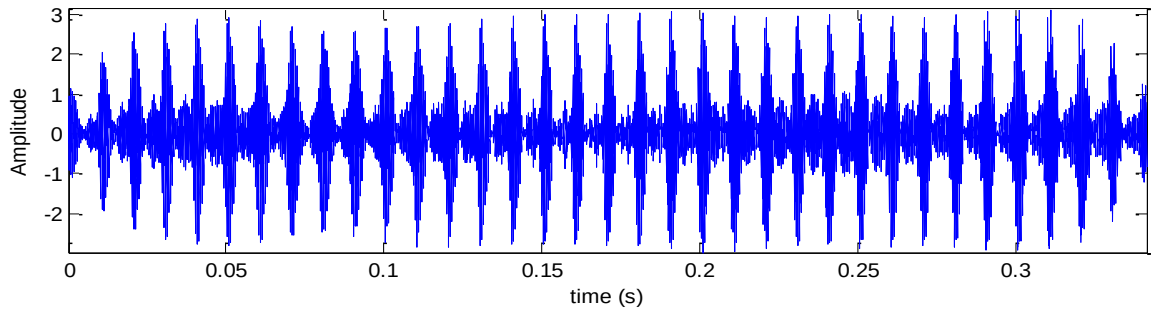

Figure 3.3: Filtered signal

3 Experimental study

3.1 Experimental system

In this study, the data used were obtained from the bearing database of Case Western Reserve University [86]. The experimental setup is shown in Figure 3.4. The test bench mainly consists of an electric motor connected to a torque transducer, which is coupled to a generator. Vibration data were collected using an accelerometer mounted on the housing with a magnetic base. The unit of measurement is mm/s² (gravity), and the duration of each vibration signal is 10 seconds. Vibration data were recorded at a sampling rate of 12000 samples per second, under four different bearing conditions:

(1) Bearing without defect (Normal condition (N));

(2) Bearing with Outer Race Fault (ORF);

(3) Bearing with a Ball Fault (BF); and

(4) Bearing with Inner Race Fault (IRF).

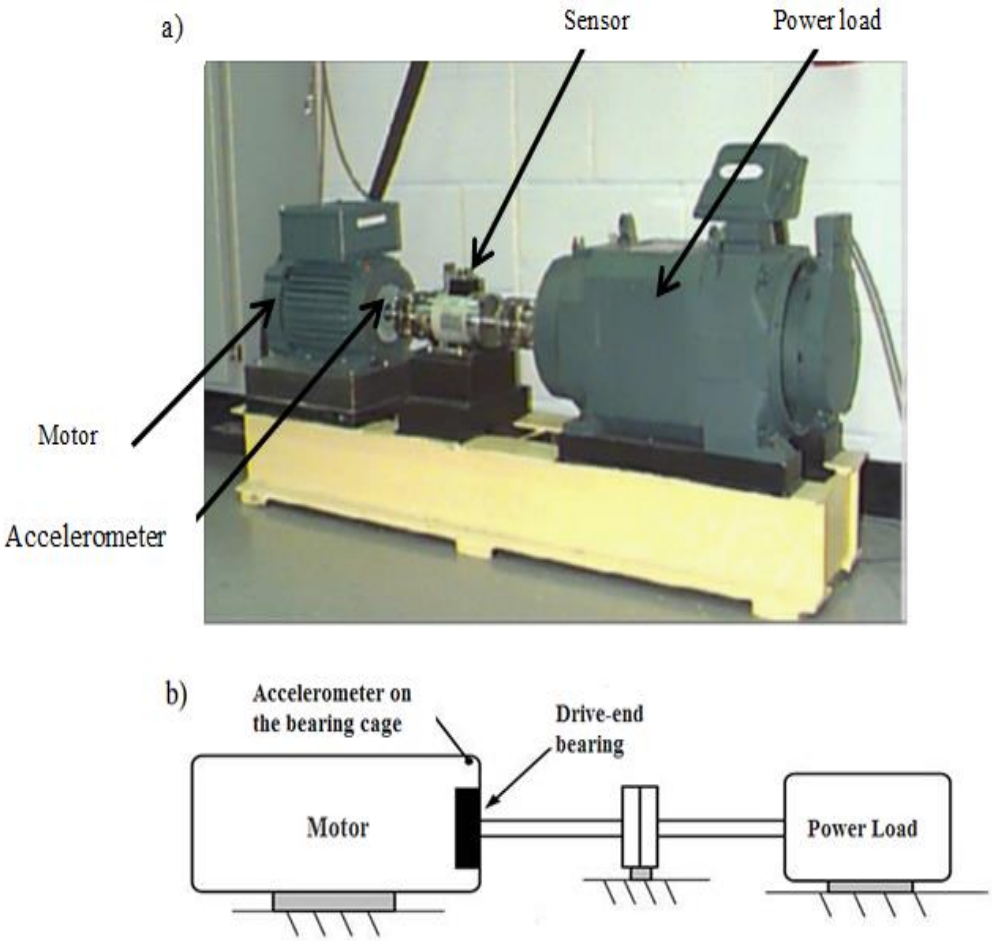

Figure 3.4: (a) Test bench of experimental system and (b) Schematic description

The defects created on the inner race and the balls have diameters of 0.1778 mm, 0.3556 mm, and 0.5334 mm, respectively. On the outer race, the defect diameters are 0.1778 mm and 0.5334 mm. The depth of all defects is 0.2794 mm. The tests were carried out under four different load conditions: 0, 1, 2, and 3 hp (horse power). Experimental measurements were collected at four distinct speeds: 1730, 1750, 1772, and 1797 rpm, which correspond approximately to 28.8, 29.1, 29.5, and 30 Hz, respectively.

Figure 3.5 shows the first 4096 samples of the vibration signals for the normal condition and the various faulty conditions, with a defect diameter of 0.5334 mm and a rotational speed of 1797 rpm (30 Hz).

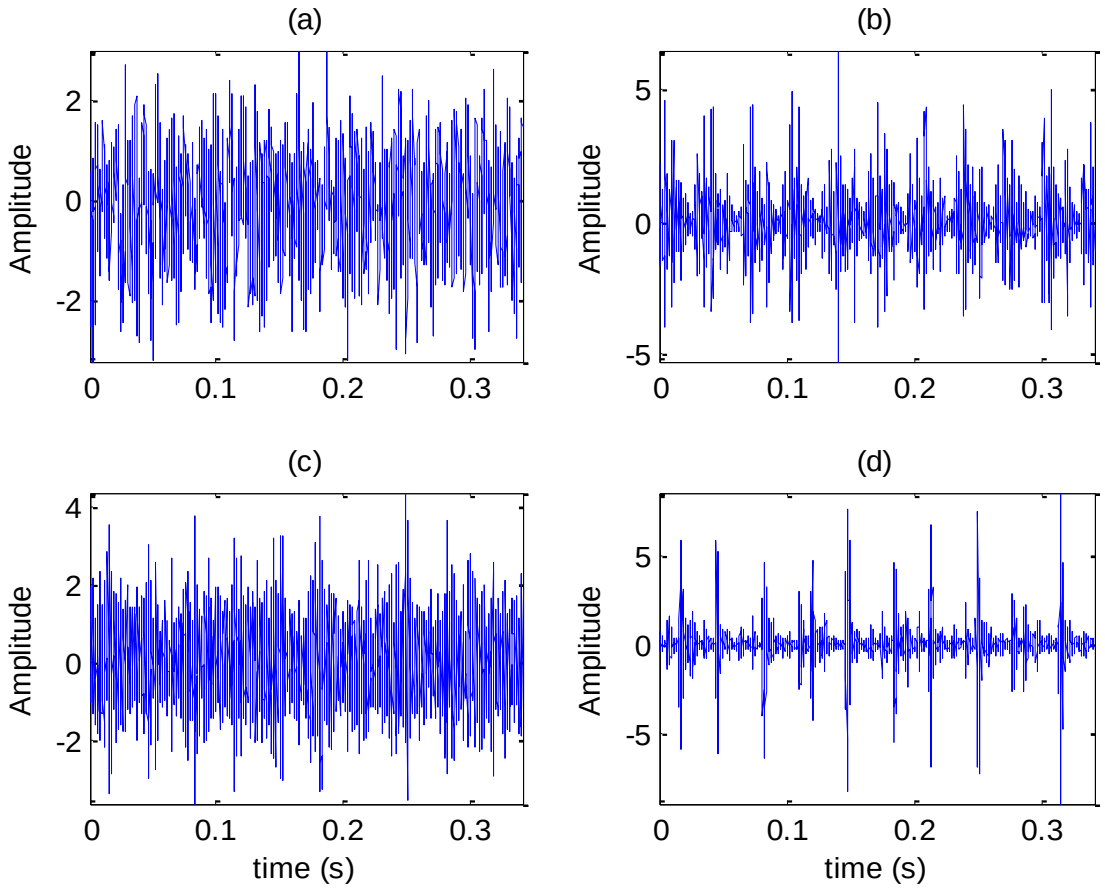

Figure 3.5: Vibration signals measured at 1797 rpm; healthy bearing (a) and bearing with a 0.5334 mm diameter defect on IR (b), B (c), and OR (d)

3.2 Results and discussion

To evaluate the effectiveness of the proposed method, it is applied to vibration signals from bearings with inner race, ball and outer race faults, as presented in Figure 3.6, 3.7 and 3.8. The objective is to assess its ability to detect faults and accurately identify their sources.

The proposed procedure is applied to retrieve the impulsive components masked within vibration signals generated from bearing defects. In the first step, the MED technique is implemented to estimate an inverse filter FIR that enhances the characteristic impulses. The

signal is truncated to a fixed size of 4096 samples, and the MED algorithm is then applied iteratively: the filter is initialized and updated at each iteration by maximizing the kurtosis of the output signal. A Toeplitz matrix derived from the autocorrelation function is used to regularize the filter computation, and the iterations continue until the change in kurtosis becomes negligible. At the end of this process, an optimal FIR filter is obtained.

In the second step, the estimated filter is used as a convolution kernel in a regularized VC algorithm. The objective is to solve the inverse problem corresponding to the convolution of an unknown signal with the estimated MED filter. To achieve this, the associated convolution matrix is constructed, and a quadratic regularization term is introduced using a 64th-order high-pass FIR filter, with the cutoff frequency specified by the user. The iterative algorithm minimizes a quadratic cost function that combines the mismatch between the measured data and its reconstruction with a penalty term related to the frequency content of the estimated signal. The impulsive signal reconstruction is updated at each iteration, and the algorithm finishes when a stopping criterion based on the norm of variation is satisfied.

Finally, the original signals, along with those obtained after MED-VC deconvolution approach, are normalized and plotted to visually assess the effectiveness of the deconvolution method. The resulting kurtosis values confirm the enhancement of the characteristic impulses, thereby validating the proposed strategy for bearing fault diagnosis.

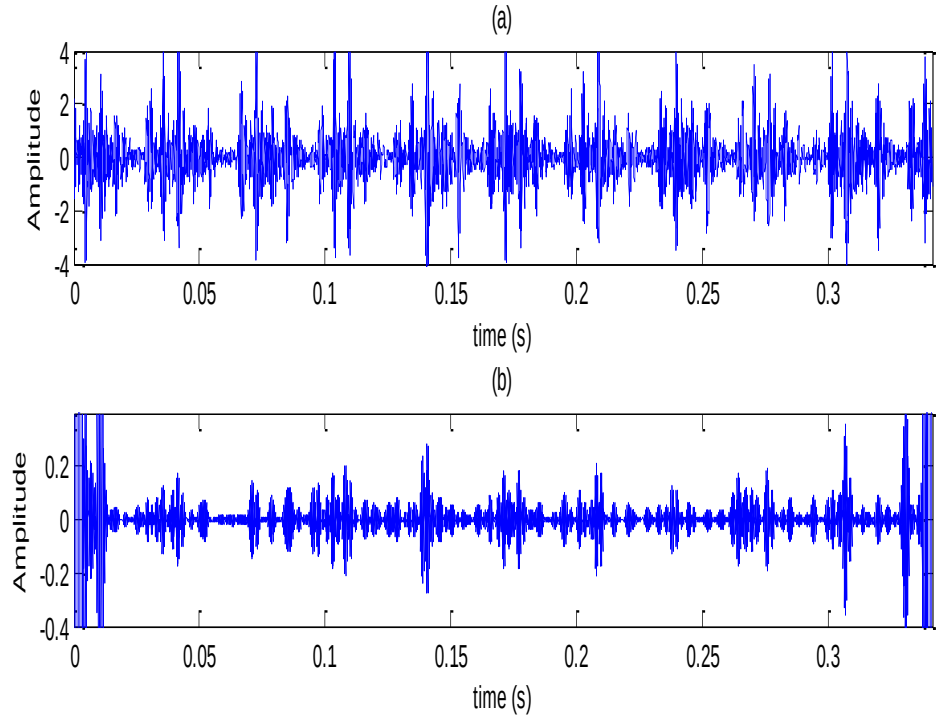

Figure 3.6: **a)** Vibration signal of bearing with fault diameter of 0.5334 mm on inner race, and **b)** filtered signal

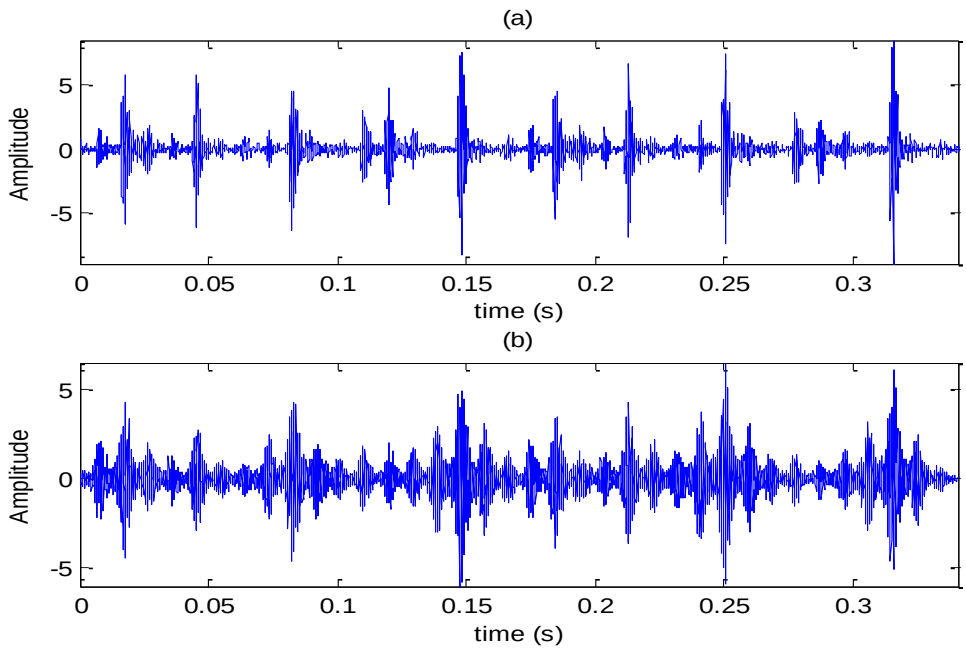

Figure 3.7: **a)** Vibration signal of bearing with fault diameter of 0.5334 mm on outer race, and **b)** filtered signal

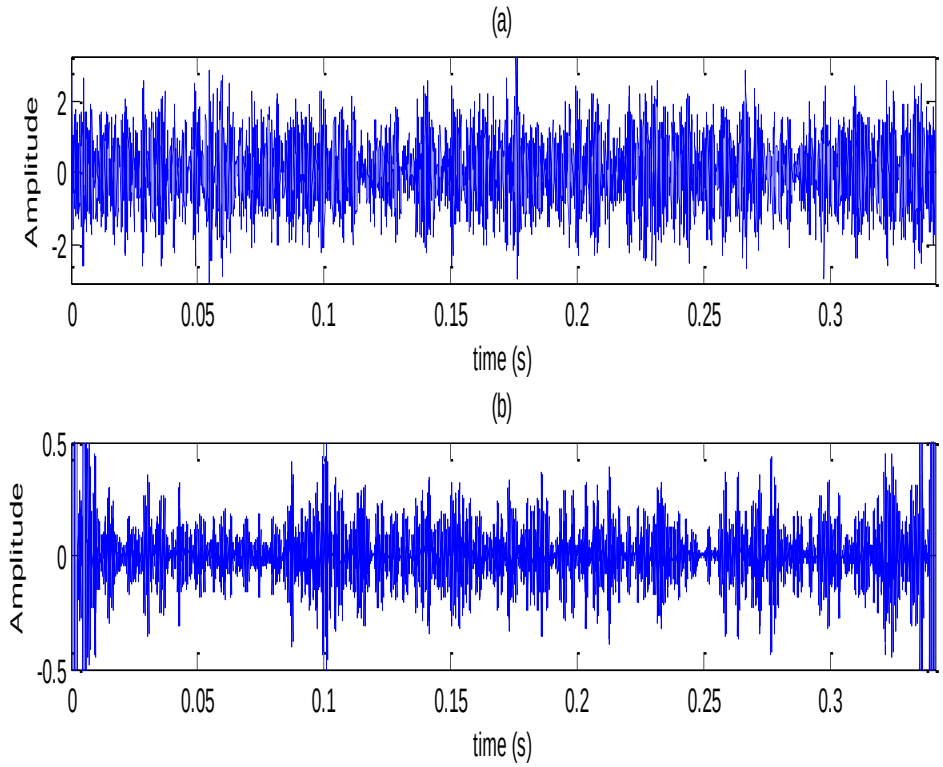

Figure 3.8: **a)** Vibration signal of bearing with fault diameter of 0.1778 mm on ball, and **b)** filtered signal

The filter length was optimized and set to 64, as this value maximized the kurtosis, as shown in Figure 3.9. This evaluation was conducted using the vibration signal from a bearing with IRF of 0.5334 mm in diameter.

Compared with the measured input signal, the periodic appearance of bearing impulses over time becomes clearly evident. To more assess the effectiveness of the proposed approach, the corresponding kurtosis values are presented in Table 3.1 and illustrated in Figure 3.10.

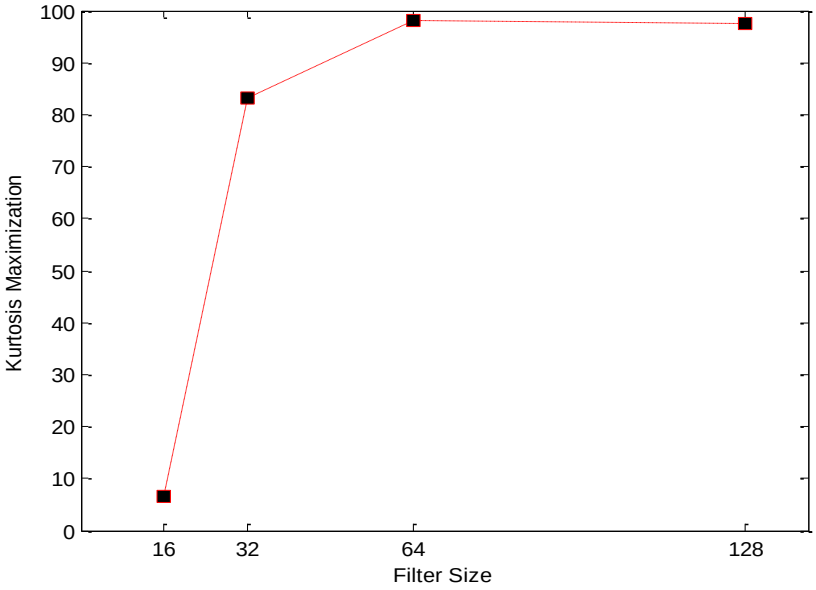

Figure 3.9: Effect of filter size on the maximization of Kurtosis

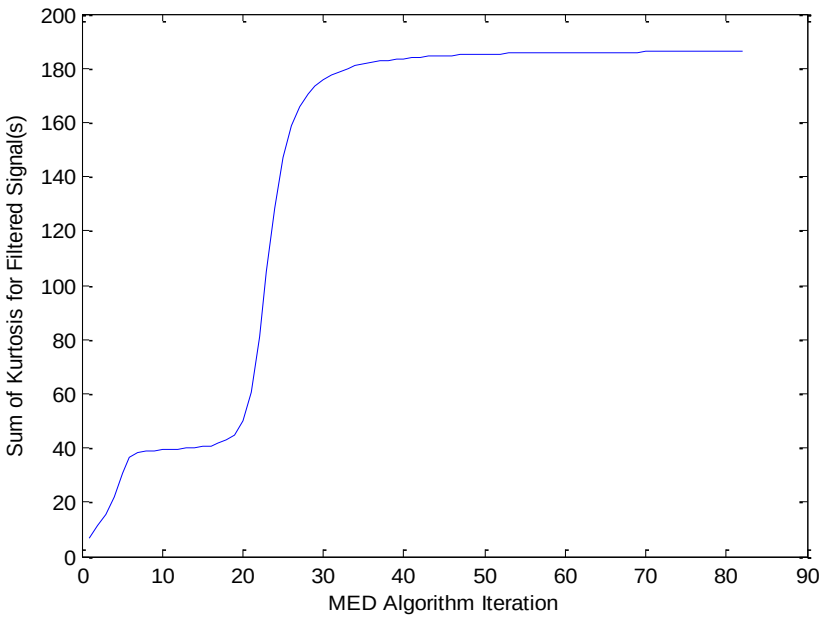

Figure 3.10: Kurtosis maximization during MED algorithm iteration

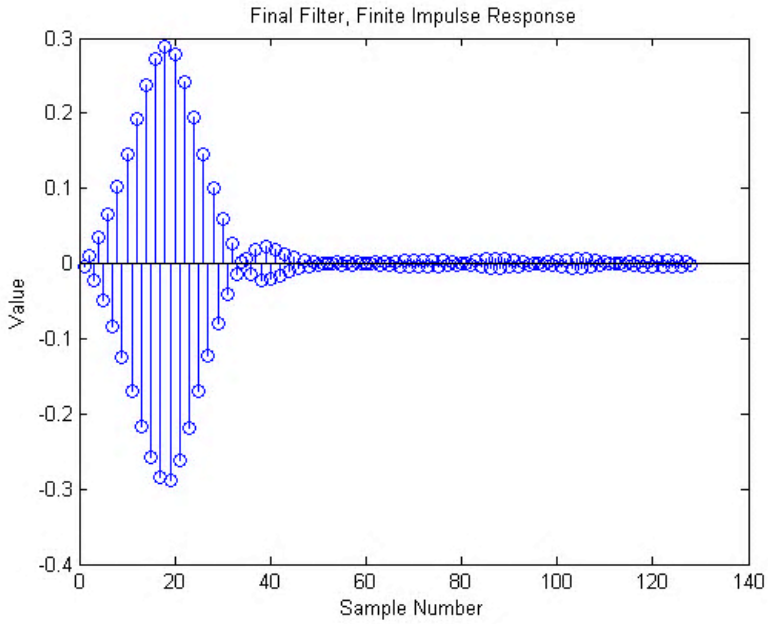

Figure 3.11: Final filter FIR

The results demonstrate that the extracted signal, which exclusively represents the characteristics of the rolling bearing faults, is accurately reconstructed.

Table 3.1: Kurtosis of filtered signals

Bearing faults	BIRF	BORF	BBF
Fault size	0.5334 mm		0.1778 mm
Input signal	6.8718	4.4488	2.6767
Filtred signal	98.1651	5.5134	102.9748

The results presented in the table reveal a clear distinction between the raw input signal and the processed output for both tested rotational speeds (1797 and 1750 rpm), indicating that the enhanced signals contain more fault-specific information. For each speed, the extracted signal characteristics were reconstructed and illustrated in Figures 3.6, 3.7, and 3.8. In particular, Figures 3.7 and 3.8 display vibration signals from bearings exhibiting IRF and BF, respectively, recorded at 1797 rpm and 1750 rpm. These figures reveal periodic impulses in the time domain,

corresponding to repeated impacts as the rolling elements interact with localized defects. The resulting impulse peaks clearly highlight the presence of faults.

The performance and convergence behavior of the MED algorithm are then demonstrated in Figures 3.10, where the sum of the kurtosis values of the filtered signals is plotted as a function of the iteration number. A sharp rise in the kurtosis sum is observed in the early iterations, typically between iterations 10 and 30, reflecting the algorithm's ability to progressively enhance the sparsity and impulsiveness of the signal. The stabilization reached around iteration 50 indicates convergence to an optimal filter. Finally, the filter obtained at convergence, corresponding to the inverse filter in the convolution model, is shown in Figure 3.11. This FIR filter exhibits a symmetric, oscillatory shape with decaying amplitude, which is characteristic of an inverse system response tailored to suppress the smearing effects of the original convolution process. Its design effectively restores the sharp transients in the signal, enabling more accurate localization and identification of fault-induced impulses.

The integrated approach yields superior results in terms of noise reduction and fault feature detection. The analysis confirms that the proposed methodology effectively extracts informative features from bearing vibration signals.

Overall, the suggested strategy proves capable of detecting the characteristic frequencies associated with damaged bearings, including BF, IRF, and ORF, outperforming earlier approaches. While different studies directly filtered the raw signal to extract diagnostic features, the proposed technique incorporates an essential preliminary step; the extraction of an inverse filter which significantly enhances the accuracy and reliability of both fault detection and signal interpretation.

4 Conclusion

This chapter demonstrated the performance of the proposed MED-VC strategy for bearing fault diagnosis using both simulated and experimental data. The simulation study confirmed the method's ability to recover periodic impulsive components even under strong noise contamination. Experimental results from the CWRU dataset further showed that the approach effectively enhances the characteristic transients associated with inner race, outer race, and ball defects.

By constructing an MED-based inverse filter and refining the reconstruction through the VC algorithm, the method produced signals with clearer impulsive features and higher kurtosis values. Overall, the proposed procedure successfully extracts fault-related information and provides reliable identification of bearing defects across different operating conditions.

General Conclusion and perspectives

In modern industrial systems, particular attention is devoted to machine–converter assemblies, where rotating machines play a crucial role. Among their components, rolling bearings are widely used and carry most of the mechanical load during operation. Their deterioration can lead to serious malfunctions, reduced production efficiency, and significant economic losses. Detecting bearing faults reliably is therefore essential. However, the impulsive signatures generated when a rolling element encounters a defect are often of very short duration and are typically embedded within noise, mechanical interferences, and modulations introduced by the transmission path. As a result, extracting these impulses with sufficient clarity remains a major challenge, especially in converter-fed machines where the vibratory environment is particularly complex.

To address these difficulties, this thesis has proposed a mathematically grounded methodology for enhancing fault-related components in vibration signals by formulating the problem as a deconvolution task. The approach combines MED, which constructs an initial inverse filter by maximizing the kurtosis of the recovered signal, with the VC iterative algorithm embedded within a regularization framework. This combined MED–VC strategy progressively improves the reconstruction of the signal, suppressing irrelevant components while preserving the impulsive features associated with bearing faults. In doing so, the method effectively handles the instability and non-uniqueness inherent to the ill-posed inverse problem that arises when directly inverting the convolution equation governing vibration signal propagation.

The methodology has been validated on both simulated and experimental data representing common bearing defects, including faults on the inner race, outer race, and rolling element. Performance evaluation using the statistical indicator ‘kurtosis’ demonstrated the ability of the proposed approach to significantly isolate the impulsive signal even under adverse measurement conditions, where noise and structural interferences considerably obscure the raw vibration signals. The substantial improvement in the clarity of the extracted impulses further confirms the robustness and effectiveness of the combined MED–VC strategy.

From an applied mathematics perspective, this work contributes to the field of inverse problems in signal processing by integrating concepts from entropy minimization, iterative

deconvolution, and regularization theory into a coherent diagnostic framework. This makes it particularly suitable for industrial environments where complete system models are rarely available and where diagnostic tools must remain both reliable and easy to deploy.

The results obtained in this thesis open several promising avenues for future research. Potential extensions include the integration of adaptive or machine-learning-based regularization schemes to automatically adjust to varying noise levels or operating conditions, the development of real-time implementations for online monitoring applications, and the use of more advanced sensing technologies to further improve measurement quality. In addition to bearing diagnosis, the proposed methodology may also be extended to other rotating machinery components where fault signatures exhibit impulsive characteristics.

This thesis contributes to advancing vibration-based fault diagnosis in converter-fed rotating machines by providing a robust and mathematically principled approach for extracting fault-related impulses in noisy environments. The framework developed herein demonstrates the significant potential of inverse problem methodologies for industrial predictive maintenance and opens the way for further progress in intelligent condition monitoring systems.

Bibliography

[1] M. Z. Ali, M. A. Matin, and M. R. I. Sheikh, “Adaptive regularization for fault detection in vibration signals: An empirical study,” *Mechanical Systems and Signal Processing*, vol. 150, 2021.

[2] Association Française de Normalisation (AFNOR). (2002). Norme X 60-010: Maintenance industrielle.

[3] BAGHLI Lotfi, " Contribution à la commande de la machine asynchrone, utilisation de la logique floue, des réseaux de neurones et des algorithmes génétiques," Thèse présentée pour l’obtention du titre de doctorat à l’université Henri Poincary, Nancy I, en génie électrique – 1999.

[4] Baraket, N., & Saidi, L. (2024). Enhanced Regularized Deconvolution in Rotating Machine Fault Detection. *Journal of Vibration and Control*. (Accepted/In Press).

[5] T. Barszcz, and N. Sawalhi, ”Fault detection enhancement in rolling element bearings using the minimum entropy deconvolution”,Arch. Acoust., 37(2) (2012), 131--141.

[6] Barszcz, T., & Urbanek, J., Application of Minimum Entropy Deconvolution to Localize Cracks in Rotating Machinery. *Key Engineering Materials*, 588 (2016), 287–294.

[7] Bendjama, H., & Boucherit, M. S. (2016). Wavelets and Principal Component Analysis Method for Vibration Monitoring of Rotating Machinery. Journal of Theoretical and Applied Mechanics, 54(2), 659-670.

[8] Bendjama, H. (2022). Bearing fault diagnosis based on optimal Morlet wavelet filter and Teager-Kaiser energy operator. Journal of the Brazilian Society of Mechanical Sciences and Engineering, 44(9), 1-23.

[9] Bianchini, C., Immovilli, F., Cocconcelli, M., Rubini, R., & Bellini, A. (2011). Fault detection of linear bearings in brushless AC linear motors by vibration analysis. IEEE Transactions on Industrial Electronics, 58(5), 1684-1694.

[10] Bolaers, F., Dron, J. P., & Rasolofondraibe, L. (2003). Prédiction et suivi de l‘évolution d‘un écaillage de fatigue de roulement par analyse vibratoire. In XVIème Congrès Français de mécanique, Nice, référence 649.

[11] A. H. Bonnet, “Cause and analysis of stator and rotor failures in threephase squirrel-cage induction motors,” IEEE Trans. Ind. Appl., vol. 28, no. 4, pp. 921–437, Jul./Aug. 1992.

[12] A. H. Bonnett and C. Yung, "Increased Efficiency Versus Increased Reliability," *Industry Applications Magazine, IEEE*, vol. 14, pp. 29-36, 2008.

[13] Bouhali, R., Tadjine, K., Bendjama, H., & Saadi, M. N. (2020). Fault diagnosis of bladed disc using wavelet transform and ensemble empirical mode decomposition. Australian Journal of Mechanical Engineering, 18, 165-175.

[14] Boulakroune M. et al 2007 Jpn. J. Appl. Phys. 46 7441. doi 10.1143/JJAP.46.7441.

[15] Boulenger A. & Pachaud C. (1998). Diagnostic vibratoire en maintenance préventive. Dunod.

[16] Brenneur, C. (2002). Eléments de maintenance préventive de machines tournantes dans le cas de défaut combinés d'engrenages et de roulements (Doctoral dissertation, L'institut national des sciences appliquées de Lyon, INSA).

[17] Chandra, D. S., & Rao, Y. S. (2019). Fault diagnosis of a double-row spherical roller bearing for induction motor using vibration monitoring technique. Journal of Failure Analysis and Prevention, 19(4), 1144-1152.

[18] Chatelain Jean, "Traité d'électricité, " Tome 1, Presse polytechniques Romandes -1983.

[19] B. Chen, W. Zhang, D. Song, and Y. Cheng, "Blind deconvolution assisted with periodicity detection techniques and its application to bearing fault feature enhancement", Measurement, 159(2020) (2020),.107804.

[20] Y. Cheng, B. Chen, and W. Zhang. "Adaptive multipoint optimal minimum entropy deconvolution adjusted and application to fault diagnosis of rolling element bearings",IEEE sensors journal, 2019, vol. 19, no. 24, pp. 12153-12164.

[21] Cherrad, M. L., Bendjama, H., & Fortaki, T. (2021). Vibration analysis for defective bearings by blind source separation. In 2021 International Congress of Advanced Technology and Engineering (ICOTEN) (pp. 1-4). IEEE.

[22] Cousinard, O. (2002). Contribution à l'étude et au développement d'un système intégré de suivi de l'endommagement des composants mécaniques sur les machines tournantes : Application au développement et au choix des outils d'analyse et de mesure vibratoire (Doctoral dissertation, Université de Reims).

[23] Daher, A. (2018). Diagnostic et pronostic des défauts pour la maintenance préventive et prédictive. Application à une colonne de distillation [Doctoral dissertation].

[24] Dahraoui, N., Bendada, A., et al. (2023). Multirésolution Deconvolution for SIMS Depth Profiling of Doped Silicon. *Journal of Applied Surface Science*, 625, 157013.

[25] Deb Majumder, B., Roy, J. K., & Padhee, S. (2019). Recent advances in multifunctional sensing technology on a perspective of multi-sensor system: a review. IEEE Sensors Journal, 19(4), 1204-1214.

[26] Djebili, O. (2013). Contribution à la maintenance prédictive par analyse vibratoire des composants mécaniques tournants. Application aux butées à billes soumises à la fatigue de contact de roulement. PhD thesis, Université de Reims.

[27] Dragomiretskiy, K., & Zosso, D. (2014). Variational Mode Decomposition. *IEEE Transactions on Signal Processing*, 62(3), 531–544.

[28] Dron J.P. (1995). Elaboration et adaptation d'outils pour l'étude et le suivi de l'endommagement de composants mécaniques par analyse vibratoire [Doctoral dissertation, Université de Reims].

[29] Dron J.P., Rasolofondraibe L., Bolaers F., & Pavan A. (2001). High-resolution methods in vibratory analysis: application to ball bearing monitoring and production machine. IJSS, 38, 4293-4313.

[30] H. Endo, R. B. Randall, “Enhancement of autoregressive model based gear tooth fault detection technique by the use of minimum entropy deconvolution filter”, Mech. Syst. Signal Process, 21(2) (2007),906--919.

[31] Farag, K. O., & Gaouda, A. M. (2012). Dynamic wavelet-based tool for gearbox diagnosis. Mechanical Systems and Signal Processing, 26, 190-204.

[32] Glowacz, A., Tadeusiewicz, R., Legutko, S., et al. (2021). Fault diagnosis of angle grinders and electric impact drills using acoustic signals. Applied Acoustics, 179, 108070.

[33] Gouri, N., Bendjama, H., & Mihoub, M. L. (2025). Combination of minimum entropy deconvolution method and Van Cittert algorithm for features extraction of bearings. ITEGAM-JETIA, 11(52), 165-172. https://doi.org/10.5935/jetia.v11i52.1569

[34] S. Gusia, " Modélisation des systèmes électroniques de puissance à commande MLI Application aux actionnements électriques, " Université catholique de Louvain, Thèse de doctorat – 2005.

[35] A. Had, K. Sabri, “A two-stage blind deconvolution strategy for bearing fault vibration signals”, Mech. Syst. Signal Process., 134 (2019),. 106307.

[36] J. Hadamard, Lecture note on Cauchy’s problem in linear partial differential equations. Yale Uni Press. 1923 [37] P. C. Hansen, “Regularization Tools: A Matlab Package for Analysis and Solution of Discrete Ill-Posed Problems,” Numerical Algorithms, vol. 6, no. 1, pp. 1–35, 1994.

[38] Harting, D. R. (1992). Demodulated Resonance Analysis-A Powerful Incipient Failure Detection Technique. ISA Transactions, 17(1)

[39] Huang, N. E., et al. (1998). The Empirical Mode Decomposition and the Hilbert Spectrum for Nonlinear and Non-Stationary Time Series Analysis. *Proceedings of the Royal Society A*, 454(1971), 903–995.

[40] Hyvärinen, A., Karhunen, J., & Oja, E. (2001). *Independent Component Analysis*. Wiley.

[41] A. Ibrahim, "Contribution au diagnostic de machines électromécaniques : Exploitation des signaux électriques et de la vitesse instantanée," Thèse de doctorat, Ecole Doctorale Sciences, ingénierie, santé, Université Jean Monnet, France, 10Mars 2009.

[42] Jalan, A. K., & Mohanty, A. R. (2009). Model based fault diagnosis of a rotor-bearing system for misalignment and unbalance under steady-state condition. Journal of Sound and Vibration.

[43] R. Jiang, J. Chen, G. Dong, T. Liu, and W. Xiao, “The weak fault diagnosis and condition monitoring of rolling element bearing using minimum entropy deconvolution and envelop spectrum”, Proc. Inst. Mech. Eng., Part C, 227(5) (2013), 1116–1129.

[44] Joseph, E. R., Jakir, H., Thangavel, B., Nor, A., Lim, T. L., & Mariathangam, P. R. (2024). Tool-Emitted Sound Signal Decomposition Using Wavelet and Empirical Mode Decomposition Techniques—A Comparison. *Symmetry*, 16(9), 1223.

[45] Kass, S. (2019). Diagnostic vibratoire autonome des roulements. (Doctoral dissertation, Université de Lyon ; Université libanaise).

[46] Kostek, R., & Żółtowski, B. (2015). Rolling bearing defect detection and diagnostics. Vibroengineering Procedia, 6, 39-144.

[47] Kerroumi, S. (2016). Extraction des paramètres et classification dynamique dans le cadre de la détection et du suivi de défaut de roulements. (Doctoral dissertation, Université de Reims Champagne-Ardenne).

[48] Kumar, A., Berrouche, Y., Zimroz, R., et al. (2023). Non-parametric Ensemble Empirical Mode Decomposition for Extracting Weak Features to Identify Bearing Defects. *arXiv preprint*, arXiv:2309.06003.

[49] Larsen, Y., & Hanssen, A. (2000). Wavelet-polyspectra: analysis of non-stationary and non-Gaussian/nonlinear signals. In Proceedings of IEEE Workshop on Statistical Signal and Array Processing (pp. 14-16).

[50] J. Li, M. Li and J. Zhang, "Rolling bearing fault diagnosis based on time-delayed feedback monostable stochastic resonance and adaptive minimum entropy deconvolution", J. Sound Vib., 401 (2017), 139—151.

[51] Liang, M., & Faghidi, H. (2014). An enhanced energy operator for bearing fault detection. In Proceedings of the 3rd International Conference on Mechanical Engineering and Mechatronics, Prague, Czech Republic (pp. 14-15).

[52] Loparo, K. A., Adams, M. L., Lin, W., Abdel-Magied, M. F., & Afshari, N. (2000). Fault detection and diagnosis of rotating machinery. IEEE Transactions on Industrial Electronics, 47(5), 1005-1014.

[53] Liu, Y., et al. (2017). Bearing fault diagnosis using MED and improved envelope analysis. *IEEE Transactions on Industrial Electronics*, 64(1), 634–644.

[54] Liu, Y., Wang, Y., & Qin, Y. (2021). Deconvolution for Machine Fault Detection: Review and New Perspectives. *Mechanical Systems and Signal Processing*, 150, 107243.

[55] Lyu, Y., et al. (2023). Nonlinear Vibration Feature Recognition Method for Reciprocating Compressor Cylinder Based on VMD-Multifractal Spectrum. *Shock and Vibration*, 2023, 2504170.

[56] Mallat, S. G. (1999). *A Wavelet Tour of Signal Processing*. Academic Press.

[57] McDonald, G. L., Zhao, Q., & Zuo, M. J. (2012). Maximum Correlated Kurtosis Deconvolution and Application on Gear Tooth Fault Detection. *Mechanical Systems and Signal Processing*, 33, 237–255.

[58] McDonald, G. L., & Zhao, Q. (2013). Deconvolution and classification of time series features for gear fault diagnosis. *Mechanical Systems and Signal Processing*, 42(1–2), 409–420.

[59] Mancina, M., Carcaterra, A., & Sestieri, A. (2023). Iterative Deconvolution and Regularization for Enhanced Fault Feature Extraction. *Mechanical Systems and Signal Processing*, 189, 110024.

[60.] Moumene, I., & Ouelaa, N. (2022). Gears and bearings combined faults detection using optimized wavelet packet transform and pattern recognition neural networks. Int J Adv Manuf Technol, 120, 4335-4354.

[61] Narvaez, C. V. I. (2007). Diagnostic par techniques d'apprentissage floues : Conception d'une méthode de validation et d'optimisation des partitions (Doctoral dissertation, Université de Toulouse).

[62] Nicodim, M., & Gheorghiu, H. (2011). Identification of faults rolling bearings through vibration and shock impulses analysis. U.P.B. Sci. Bull., Series D, 73(1), 63-70.

[63] O. Ondel," Diagnostic par reconnaissance des formes: Application a un ensemble convertisseur – machine asynchrone," Thèse de doctorat, Ecole Centrale de Lyon, France, 2006.

[64] Ovacikli, A. K., Pääjärvi, P., & LeBlanc, J. P. (2013). Skewness as an objective function for vibration analysis of rolling element bearings. In: 8th International Symposium on Image and Signal Processing and Analysis (ISPA), 462-466. IEEE.

[65] Pekpe, K. M. (2004). Identification par les techniques des sous-espaces application au diagnostic (Doctoral dissertation, Institut National Polytechnique de Lorraine).

[66] Pennacchi, P., Borghesani, P., Chatterton, S., & Ricci, R. (2011). An experimental based assessment of the deviation of the bearing characteristic frequencies. In 6th International Conference Acoustic and Vibratory Surveillance Methods and Diagnostic Techniques, Compiegne.

[67] Sar, S. K., & Kumar, R. (2020). Hasty Fault Diagnosis of a Rotating Machinery Hinge on Stalwart Trippy Classifier with Robust Harmonized Swan Machine. Jordan Journal of Mechanical & Industrial Engineering, 14(2), 223-236.

[68] Sawalhi, N., Randall, R. B., & Endo, H. (2007). The enhancement of fault detection and diagnosis in rolling element bearings using minimum entropy deconvolution combined with spectral kurtosis. *Mechanical Systems and Signal Processing*, 21(6), 2616–2633.

[69] Sengupta, N., Sahidullah, M., & Saha, G. (2016). Lung sound classification using cepstral-based statistical features. Computers in Biology and Medicine, 75, 118-129.

[70] Shanmukha, P., Ramesh, M. R., & Naidu, VPS. (2014). Bearing Health Condition Monitoring: Frequency Domain Analysis Multi-Sensor Data Fusion. International Journal of Advanced Research in Electrical, Electronics and Instrumentation Engineering, 3(5), 260–268.

[71] Sharma, B. K., Kumar, M., & Meena, R. S. (2024). Development of a Speech Separation System Using Frequency Domain Blind Source Separation Technique. *Multimedia Tools and Applications*, 83, 32857–32872.

[72] Tandon, N., & Choudury, A. (1999). A review of vibration and acoustic measurement methods for the detection of defects in rolling element bearings. International Journal of Tribology, 32, 469-480.

[73] P. Tavner, L. Ran, J. Penman, and H. Sedding, Condition Monitoring of Rotating Electrical Machines, 2 ed. London, United Kingdom: Institution of Engineering and Technology, 2008.

[74] O. V. Thorsen and M. Dalva, "A survey of faults on induction motors in offshore oil industry, petrochemical industry, gas terminals, and oil refineries," *Industry Applications, IEEE Transactions on,* vol. 31, pp. 1186-1196, 1995.

[75] O. V. Thorsen and M. Dalva, "Failure identification and analysis for high-voltage induction motors in the petrochemical industry," *Industry Applications, IEEE Transactions on,* vol. 35, pp. 810-818, 1999.

[76] A. N. Tikhonov and V. Y. Arsenin, *Solutions of Ill-Posed Problems*, Winston & Sons, Washington, 1977.

[77] Tiwari, R., Gupta, V. K., & Kankar, P. K. (2015). Bearing fault diagnosis based on multi-scale permutation entropy and adaptive neuro fuzzy classifier. Journal of Vibration and Control, 21(3), 461-467.

[78] B. Trajin, "Analyse et traitement de grandeurs électriques pour la détection et le diagnostic de défauts mécaniques dans les entraînements asynchrones," Thèse de doctorat, l'Institut National Polytechnique de Toulouse, 1 Décembre 2009.

[79] P. H. Van Cittert, "Zum einfluss der spaltbreite auf die intensitätsverteilung in spektrallinien. Ii'', Z. Physik,vol. 69, no. 5, pp. 298-308, 1931.

[80] B. Vaseghi, "Contribution à l'étude des machines électriques en présence de défaut entre spires," Thèse de doctorat, GREEN - Groupe de Recherche en Electrotechnique et Electronique de Nancy, Nancy Université - Institut National Polytechnique de Lorraine, 2009.

[81] Wiggins, R. A. (1978). Minimum Entropy Deconvolution. In *SEG Annual Meeting*. Society of Exploration Geophysicists.

[82] Wiggins, R. A. (1978). Minimum Entropy Deconvolution. *Geoexploration*, 16(1–2), 21–35.

[83] Xin, G. (2017). Sparse representations in vibration-based Rolling element bearing diagnostics. (Doctoral dissertation, Université de Lyon).

[84] Yang, Q. (2004). Model-based and data driven fault diagnosis methods with applications to process monitoring (Doctoral dissertation, Université Case Western Reserve).

[85] Yu, J. (2012). Local and nonlocal preserving projection for bearing defect classification and performance assessment. IEEE Transactions on Industrial Electronics, 59(5), 2363-2376.

[86] Zhao, M., Lin, J., Xu, X., & Li, X. (2014). Multi-Fault Detection of Rolling Element Bearings under Harsh Working Condition Using IMF-Based Adaptive Envelope Order Analysis. Sensors, 14(11), 20320-20346.

[87] Zhao, L., Zhang, Y., & Zhu, D. (2019). Rolling element bearing fault diagnosis based on adaptive local iterative filtering decomposition and Teager-Kaiser energy operator. Journal of Failure Analysis and Prevention, 19(4), 1018-1022.

[88] J. Zhang, M. Zhong, J. Zhang, "Detection for weak fault in planetary gear trains based on an improved maximum correlation kurtosis deconvolution", Meas. Sci. Technol, vol. 31(2) (2019), 025101.

[89] Zhu, Y., Yan, Q., & Lu, J. (2020). Fault diagnosis method for disc slitting machine based on wavelet packet transform and support vector machine. International Journal of Computer Integrated Manufacturing, 33(10- 11), 1118-1128.

[90] Zhu, D., & Yin, B. (2021). Fault diagnosis method for rolling element bearing based on enhanced cross correlation spectrum. Journal of Failure Analysis and Prevention, 21(6), 2190-2201.

[91] Zoungrana, W. B., Chehri, A., & Zimmermann, A. (2020). Automatic classification of rotating machinery defects using machine learning (ml) algorithms. Human Centred Intelligent Systems, 189, 193-203.

[92] Loparo, K.A. (2016). Bearing vibration dataset, Case Western Reserve University. Available at: www.eecs.case.edu/laboratory/bearing.